Environmental Characterization and Modeling Studies to Better Understand Coastal Erosion in the Little Beach Area of Bonnet Shores, Rhode Island

Authors:

Brian Caccioppoli, Bryan A. Oakley, Reza Hashemi, Arash Rafiee Dehkharghani, John W. King

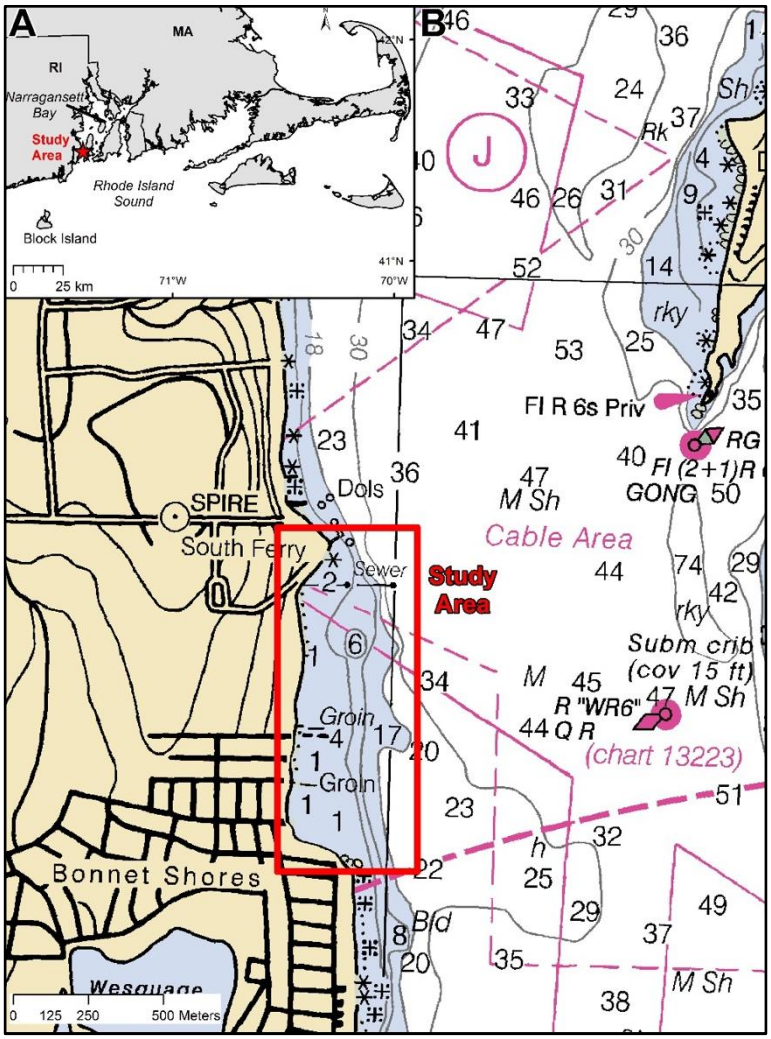

THE UNIVERSITY OF RHODE ISLAND GRADUATE SCHOOL OF OCEANOGRAPHY

EASTERN CONNECTICUT STATE UNIVERSITY

TABLE OF CONTENTS

1 Introduction

A team of researchers from The Graduate School of Oceanography and the Ocean Engineering Department at the University of Rhode Island and the Environmental Earth Sciences Department at Eastern Connecticut State University undertook a study of the Little Beach area of Bonnet Shores, Rhode Island. The objectives of the study were to fully characterize the study area by detailed mapping and modeling studies in order to enhance our understanding of coastal erosion within the study area, and to initiate an evaluation of possible erosion mitigation measures that could be undertaken in future. The study had three major components. These components included LiDAR (Light Detection And Ranging) mapping of the shoreline and proximal landward structures and landforms, sonar mapping of the benthic geologic habitat in the proximal shoreface area, and numerical modeling of erosional processes within the study area.

2 Boat-based LiDAR Surveys of the Little Beach Shoreline, Narragansett, Rhode Island

Authors: Brian Caccioppoli and John W. King

2.1 Introduction

Little Beach is a sandy beach along the west passage of Narragansett Bay, RI and used recreationally by residents and visitors of the Bonnet Shores Fire District in Narragansett, RI. Little Beach is more protected than more wave-exposed Rhode Island beaches (e.g. Narragansett Town Beach), however, it is vulnerable to accelerating sea level rise and more intense storm events that are projected to occur with increasing frequency due to global climate change. Other beaches throughout the state have a well-documented annual storm beach cycle beach cycle (Figure 2-1) (Hayes and Boothroyd, 1969; Davis et al., 1972) where beach sand volume increases during seasonal lulls in storminess (spring and summer) and decreases during more stormy seasons (fall and winter). We don't have the data to determine if Little Beach experiences this cyclic seasonal change in beach sand volume, but anectdotal evidence obtained from long-term residents of the study area indicates that Little Beach does tend to have a higher sand volume during summer conditions than it does after fall and winter storms. That is a classical storm beach cycle pattern.

Boat-based LiDAR is an evolution of stationary terrestrial laser scanning, where the former consists of mobile laser scans and the latter involves stationary laser scans with overlapping fields of view. Boat-based LiDAR has been proven as a useful technology for mapping topographic change on shoreline bluffs and beaches (e.g. Baron and Kaminsky, 2012; Kaminsky et al., 2014). University of Rhode Island Graduate School of Oceanography (URI GSO) has developed methodology for boat-based LiDAR for coastal applications and has compared the usefulness to traditional survey methods (Caccioppoli et al., 2017a, b).

URI GSO was tasked with producing baseline beach elevation data at Little Beach using a boat-based LiDAR system. The results of two surveys are reported within this document establishing beach volume estimates, elevation maps and a beach volume elevation change analysis between the two surveys. The surveys were collection in the late summer and early summer (September 9, 2020 and October 19, 2022, respectively) to reduce any seasonal influence in beach sediment volume, should an annual storm beach cycle signal exist at Little Beach.

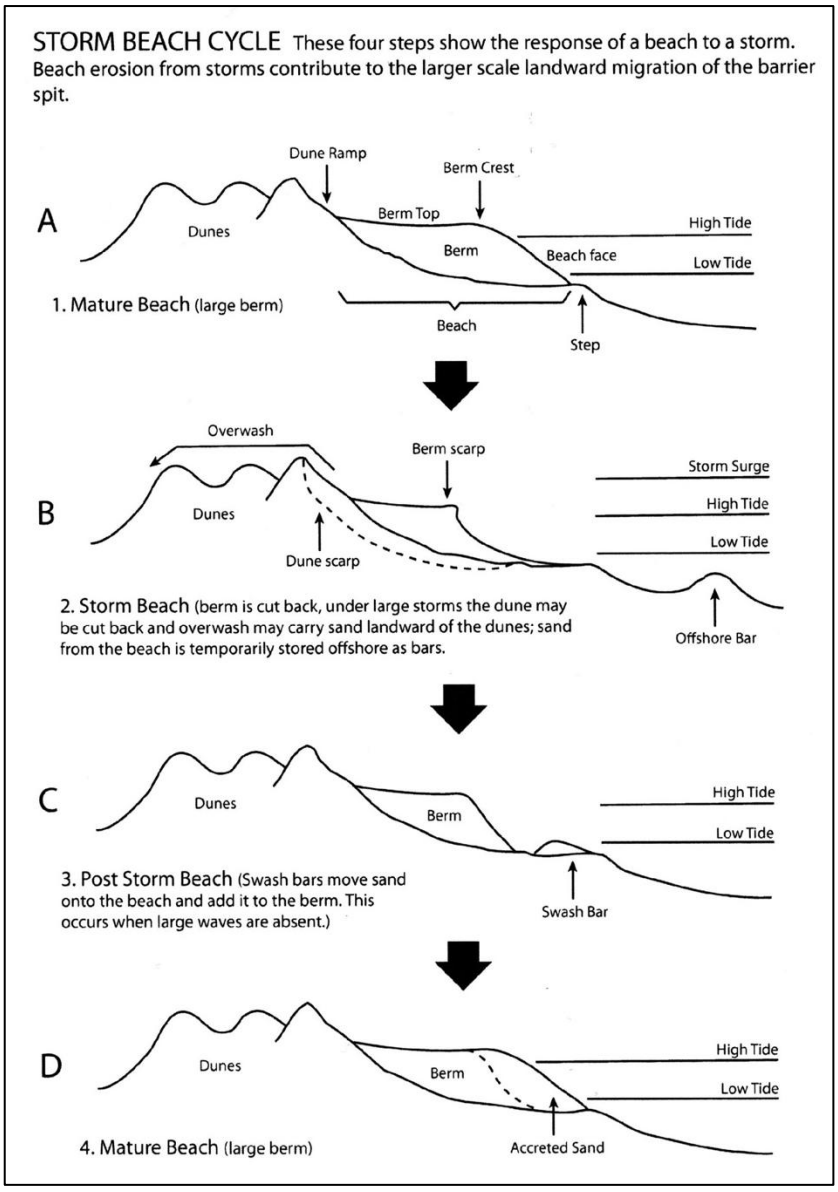

Figure 2-1. Storm Beach Cycle.
The typical phases of the storm beach cycle, beginning at a mature beach (A), typically seen in summer months in Rhode Island. The storm beach phase (B) occurs after large waves and storm surge erode the berm and dunes and are common in the Fall and Winter months. The post storm beach phase (C) occurs under low wave energy conditions, naturally replenishing the berm volume

2.2 Methodology

Boresight Calibration

A boresight calibration of the LiDAR and Inertial Measurement Unit (IMU) was conducted on March 7, 2019. This particular calibration accounts for any angular misalignments between the LiDAR and IMU systems as they are mounted on a sensor frame. Angular misalignments that are improperly

registered can result in survey inaccuracies that worsen with distance (Figure 2-2). Properly aligned systems greatly reduce the time and effort required for additional alignments in post-processing.

Surveys

The following equipment was used to carry out LiDAR scans of Little Beach (Figure 2-3):

- Teledyne-Optech ILRIS-3D motion compensated laser scanner system [Raw point and intensity data]
- Applanix POSMV IMU system [Positioning and orientation data]
- Trimble R10 RTK-enabled GNSS receiver [High-precision positioning]
- *R/V Shanna Rose* [42' survey vessel]

Boat-based LiDAR scans of Little Beach were conducted on September 9, 2020 and October 19, 2022. The survey equipment was setup on the *R/V Shanna Rose* at the URI Allen Harbor Facility the day before and the morning of each survey. The optically-safe ILRIS laser scanner (LiDAR), IMU and RTK GNSS systems were mounted on a sensor frame with known horizontal and vertical offsets. The sensor frame was fixed to the *R/V Shanna Rose*, approximately 8 feet above the deck on the starboard side.

September 9, 2020 Survey

The *R/V Shanna Rose* transited to Little Beach, arriving at 8:45 AM EDT, with surveys beginning shortly thereafter. The surveys were planned to occur in the morning to coincide with lower tidal conditions to maximize the length of the exposed beach. Low tide was predicted to occur at 6:14 AM EDT at NOAA Water Level Station 8454658 Narragansett Pier, RI. The survey date was chosen based on the favorable forecasted weather and sea conditions, which can have a noticeable impact on data quality (Figure 2-4). Seas were approximately 1-2 feet and winds were light and variable during the duration of the LiDAR scans. The calm seas and fair weather allowed the survey vessel to navigate as near to the beach as possible, allowing for the best possible data density.

October 19, 2022 Survey

The *R/V Shanna Rose* transited to Little Beach, arriving at 9:07 AM EDT, with surveys beginning shortly thereafter. Low tide was predicted to occur at 9:29 AM EDT at NOAA Water Level Station 8454658 Narragansett Pier, RI. Seas were approximately 1-2 feet and winds were 5-10 kt WSW during the duration of the LiDAR scans (Figure 2-4).

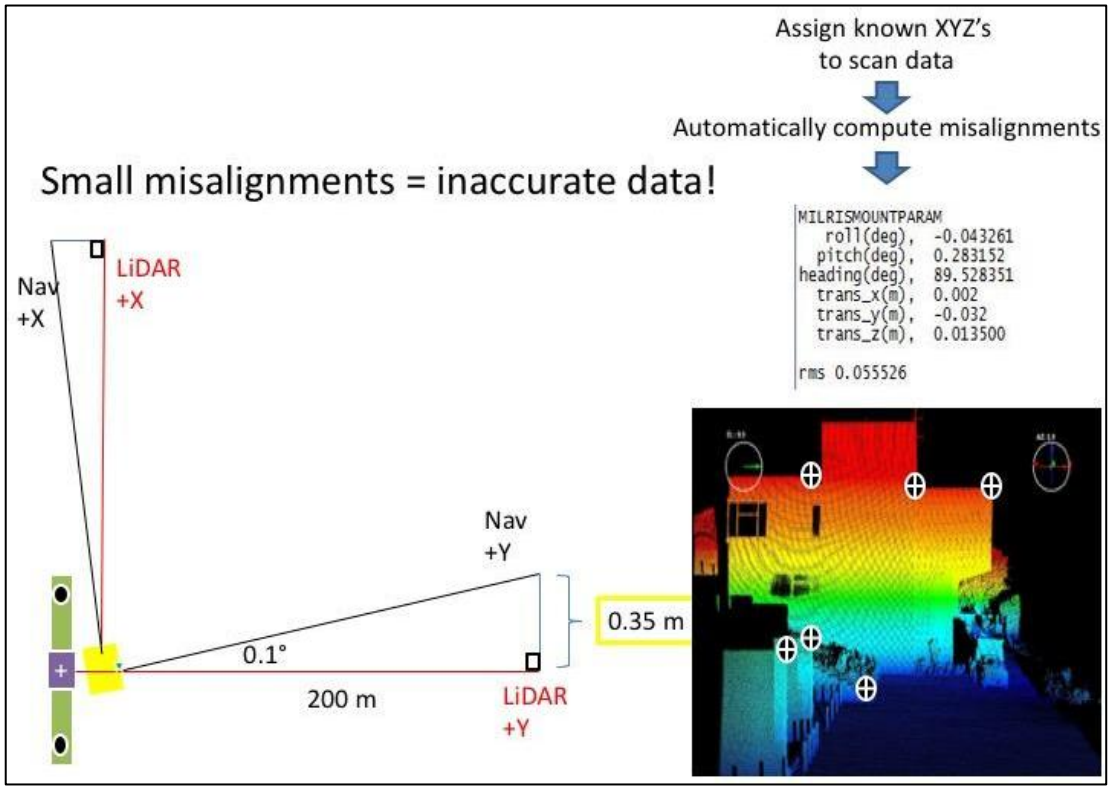

Figure 2-2. Boresight calibration
Boresight calibrations are performed prior to LiDAR survey. This ensures that the reference frames of the IMU (navigation) and LiDAR are properly aligned. The above schematic shows a resulting

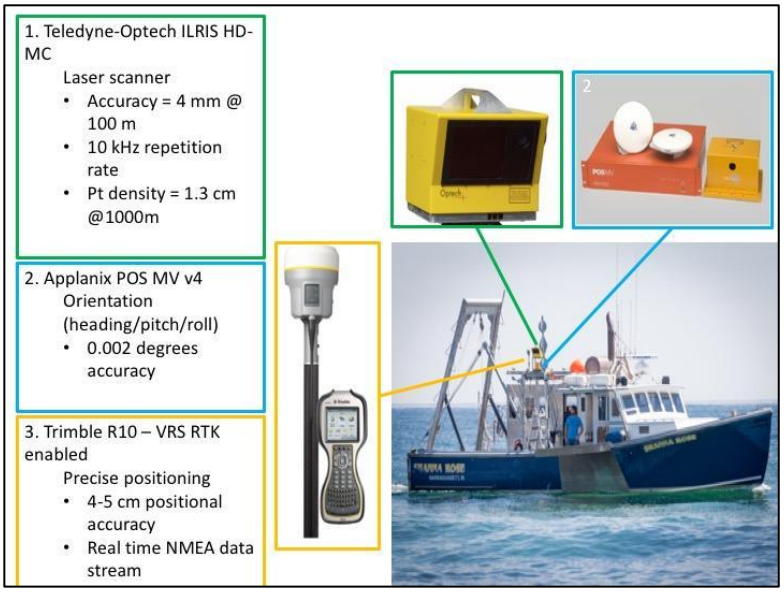

Figure 2-3. LiDAR survey components.
The LiDAR survey relies on integration of three primary components. The LiDAR system (1), the IMU (2) and an RTK enabled GPS (3). All components are mounted on a sensor frame aboard the *R/V Shanna Rose*.

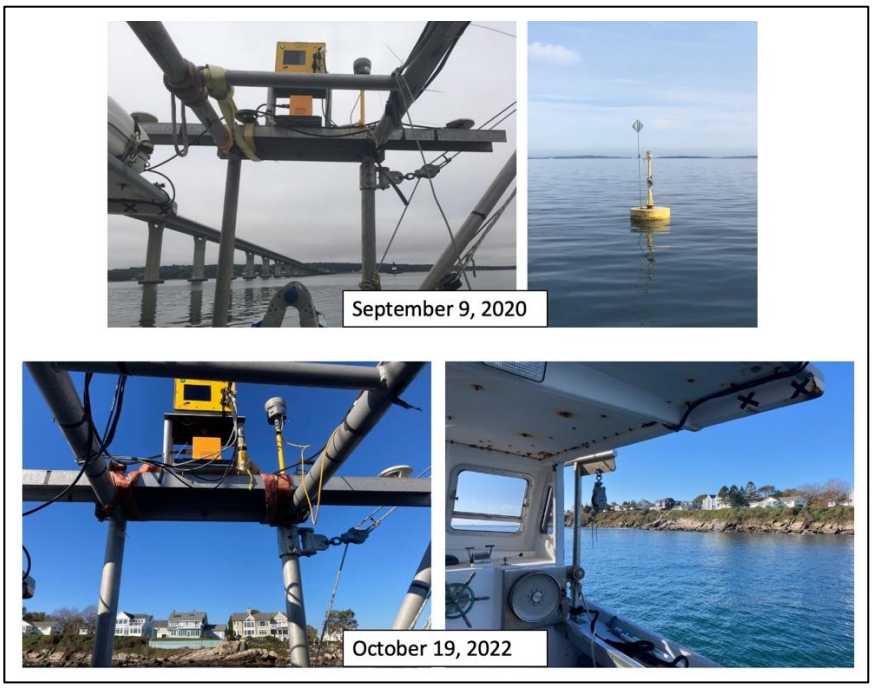

Figure 2-4. Survey conditions for September 9, 2020 and October 19, 2022.
Fair weather and a calm sea state enabled the *R/V Shanna Rose* to be navigated close to the shoreline, resulting in good data density. Surveying began near low tide when the beach is most exposed.

Shore-parallel, north-south scans were conducted along Little Beach beginning in the vicinity of URI's Bay Campus pier and concluding at the south end of the Bonnet Shores mooring field. LiDAR scan and navigation data were recorded to data acquisition laptops. The *R/V Shanna Rose* maintained survey speeds of 3 – 3.5 knots throughout each scan and generally followed the 10-foot isobath to ensure high data quality and safe navigation. Following the completion of several LiDAR scans along Little Beach, the boat was transited back towards Allen Harbor. After each scan, data were processed into a point cloud to determine if adequate resolution and data coverage along the beach were met. This method allowed the surveyor to adjust LiDAR settings to maximize data quality.

Data Processing

Generating georeferenced "xyz" point clouds

The raw LiDAR scan data was parsed with the position and orientation data using Optech Parser software. The boresight calibration values and sensor offsets are also compensated in this software. The result is a 3-D point cloud XYZ file, where each point has a real-world projected position (x and y in meters) with respect to the WGS84 horizontal datum and an elevation (z in meters) value with respect to the WGS84 ellipsoid.

Datum transformations were then made in NOAA V-Datum software. Positions were re-projected in the NAD83 UTM Zone 19N projected coordinate system and elevations were projected with respect to the NAVD88 elevation datum. The units for all positions and elevations in the point cloud are meters.

Data filtering and alignment

Cloud Compare software was used for fine-scale alignments of datasets, error analysis and manual point removal of non-bare earth topography. LiDAR point clouds from each scan were merged into a single point cloud for each survey year to maximize point density. The resulting merged point cloud datasets for September 9, 2020 and October 19, 2022 were then spatially aligned using a fine-scale georegistration technique. This alignment technique requires a user to identify matching points within the two datasets and calculation of Root Mean Squared Error (RMSE), a statistical measure of accuracy between the two datasets. The resulting RMSE for 15 alignment point matches was 0.264 meters.

The majority of the points generated by the LiDAR are returns from laser light reflections off man-made objects, such as boats in the mooring field, houses, cars and other man-made objects, none of which are useful for quantifying beach volume (Figure 2-5). Manual point removal was used to extract only points representing bare-earth topography (in this case, points only representing elevations along the beach). This process required identifying and removing points associated with people, vegetation, fencing and buildings. The finalized point cloud was then rasterized into a 1x1 m grid, using an average value interpolation for elevation (Figure 2-6). This final beach elevation raster is referred to as a digital elevation model (DEM) and was exported in GeoTIFF format (Figure 2-8, 2-9).

Geoprocessing and analysis

The DEM was then imported to ESRI ArcMap GIS software for additional geoprocessing and analysis. A polygon feature class representing the extent of the beach was produced during the The September 2020 and October 2022 DEMs were then clipped to the extent polygon (Figure 2-7). Both surveys

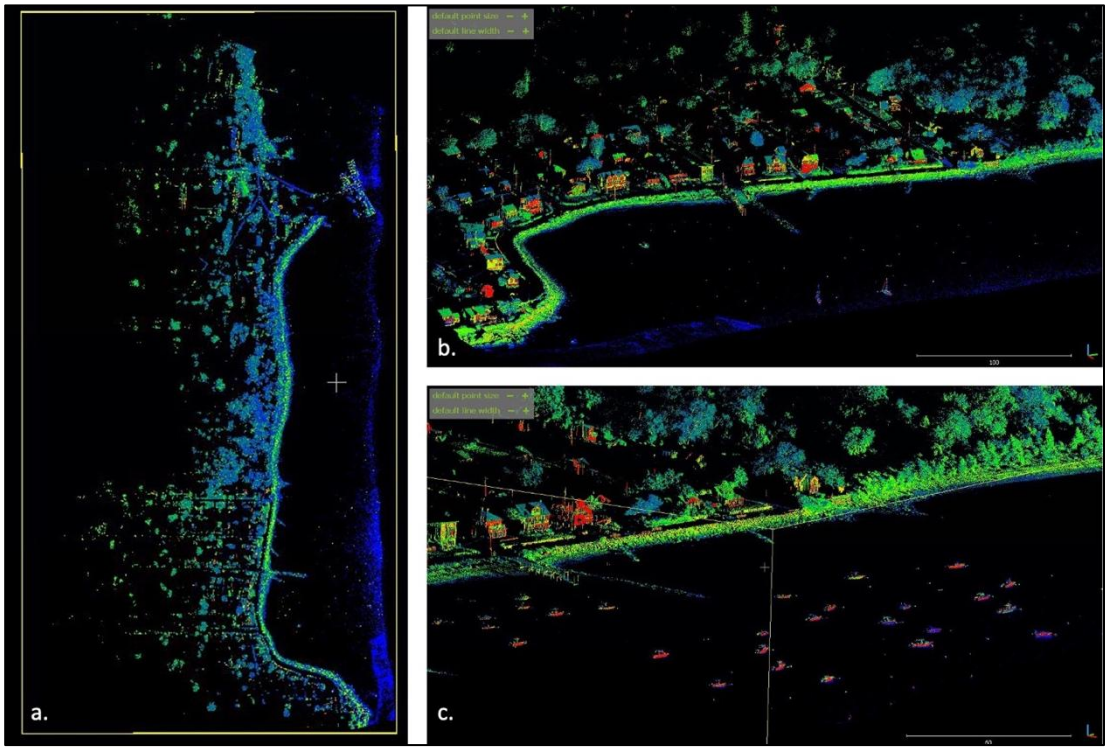

Figure 2-5. Raw point cloud data.
Scenes of raw point cloud data from Little Beach. Scene (a.) depicts the entire scan extent, including portions of URI's Narragansett Bay Campus. Scene (b.) depicts Little Beach, looking towards the west, where houses, vegetation and other man-made structures can be seen. Scene (c.) depicts the Bonnet mooring field, with moored vessels.

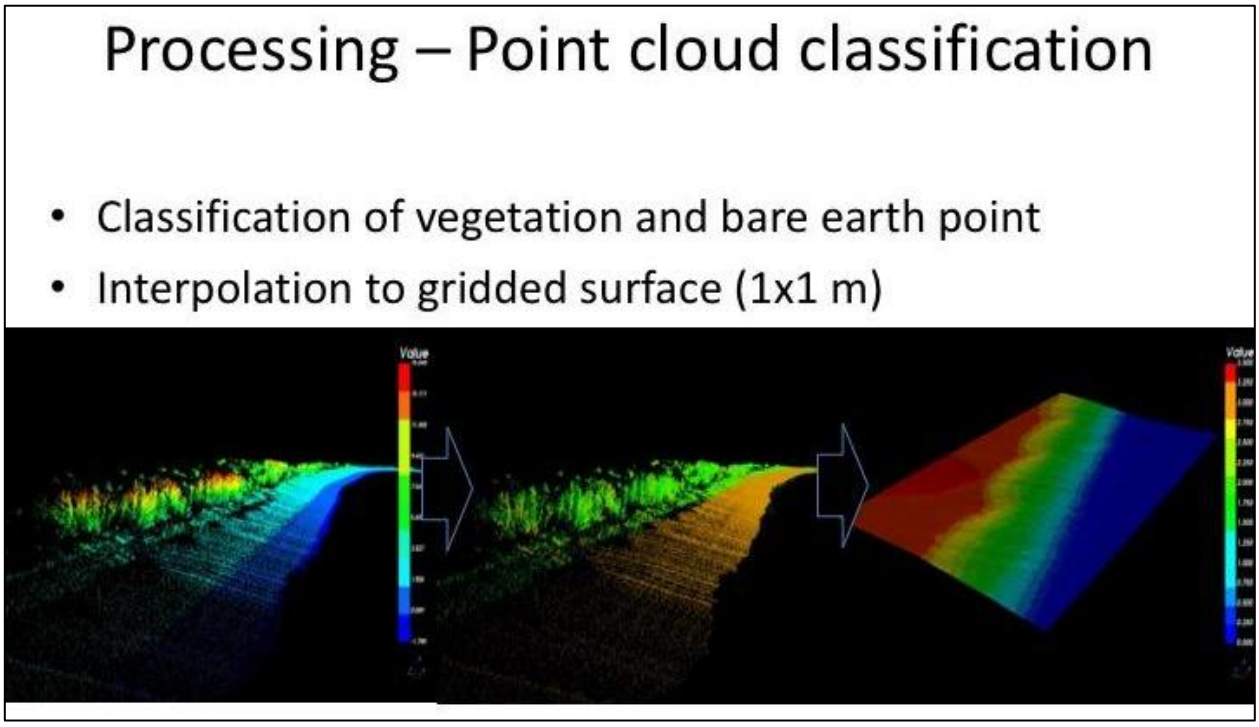

Figure 2-6. Processing of work flow.
(Left) Unedited raw point cloud data showing vegetation and beach. (Middle) Point cloud with points separated into two classes, vegetation and beach. (Right) Digital Elevation Model of the same section of beach, as a 1x1 meter gridded surface.

Figure 2-7. Data extent polygon / clip boundary
Polygon drawn in ArcMap GIS software to clip elevation datasets. Polygon ensures that the same surface area is used for analyses.

Figure 2-8. Interpolated Digital Elevation Model of Little Beach berm, September 9, 2020.
Final DEM representing only beach elevations along Little Beach. All non-bare earth points were removed before producing the 1x1 meter gridded surface.

Figure 2-9. Interpolated Digital Elevation Model of Little Beach, October 19, 2022.
Final DEM representing only beach elevations along Little Beach. All non-bare earth points were removed before producing the 1x1 meter gridded surface.

were clipped to the same extent polygon so that beach volume calculations can be performed for the same given surface area. The volume of the berm was calculated using the Surface Volume tool (3D Analyst Geoprocessing toolbox) in ArcMap. Beach volumes were then calculated above a horizontal reference plane set to 0-meter elevation (with respect to the NAVD88 vertical datum).

Change Analysis

A change analysis was identified as a useful metric for understanding how a beach has changed over time (Caccioppoli et al., 2017). This method digitally subtracts the elevations of the more recent DEM from the elevations of a previous DEM, and visually displays the changes in elevation as a new map. The map is then colorized depending on the degree of change, and whether or not the changes were positive (erosion) or negative (accretion).

The change analysis was calculated by differencing the elevations of the two DEMs (September 2020 and October 2022) at each 1-meter grid cell using the "Minus" tool in ArcMap's 3D Analyst toolbox. The resulting elevation differences were then mapped as a new raster, where each cell represents the change in elevation between the LiDAR DEMs being compared, which are then scaled to show the spatial patterns of change throughout the analysis area (Figure 2-10).

Following geological conventions where an older dataset represents the baseline to which subsequent datasets are compared, the October 2022 DEM elevations were subtracted from the older September 2020 baseline DEM. Due to this convention, cells that experience a positive elevation change value are considered as erosion (removal of beach sand), and cells with a negative elevation change value are considered as accretion (growth of beach sand). This convention is noteworthy since it may be counterintuitive to consider negative changes in elevation to represent accretion. For this reason, it is much easier to visualize changes in elevations with intuitive maps. Each cell in the change analysis raster was classified into elevation bands and an intuitive color palate was assigned to distinguish areas of erosion and accretion along the shoreline. Cells with little to no change in elevation ($\leq$ 0.25 m) are mapped as no color. Cells with positive ($>$ +0.25 m) elevation changes represent areas of erosion and are mapped with a red color palate. Cells with negative ($<$ -0.25 m) elevation change values represent areas of accretion and are mapped with a green color palate.

2.3 Results

Beach Volume

The beach volume of the Little Beach for the September 2020 survey was calculated as 6,164 cubic meters above the NAVD88 elevation datum. The volume of beach Little Beach for the October 2022 survey was calculated as 5,781 cubic meters above the NAVD88 elevation datum. The percent change in beach volume between the two surveys shown in Table 2.1 was a decrease in beach volume of 6.2%.

Table 2.1 LITTLE BEACH VOLUMES	
Date	**Volume (cubic meters, NAVD88)**
9/9/2020	6,164
10/19/2022	5,781
PERCENT CHANGE	
Date Range	**NAVD88**
9/9/2022 to 10/19/2022	-6.2%

Change Analysis – September 9, 2020 to October 19, 2022

This change analysis compares beach volumes at the same time of year, with 2 years of elapsed time between the surveys, which should account for any beach volume seasonal cyclicity such as that of the annual storm beach cycle. The timing of these surveys, in late summer to early fall, following quieter wave conditions during the summer coincide with the expected storm beach cycle volume maximum. The magnitude of volume change observed between the September 2020 and October 2022 surveys is a small decrease in beach volume, 6.21% decrease with respect to NAVD88. The timing of the October 2022 survey was slightly later in the year compared with the September 2020 survey which may have influenced the lower beach volume.

The spatial patterns of the changes in elevation between the September 2020 and October 2022 surveys are mapped in the change analysis figure (Figure 2-10). Most of this change analysis is mapped as white in color, meaning the majority of the elevation changes are +/- 0 to 0.25 m. There are some isolated areas of more than 0.5 m decrease in elevation, particularly along the road.

Areas of accretion are sparse, and sporadically distributed along the beach, with changes that are mostly <0.5 m increases in elevation.

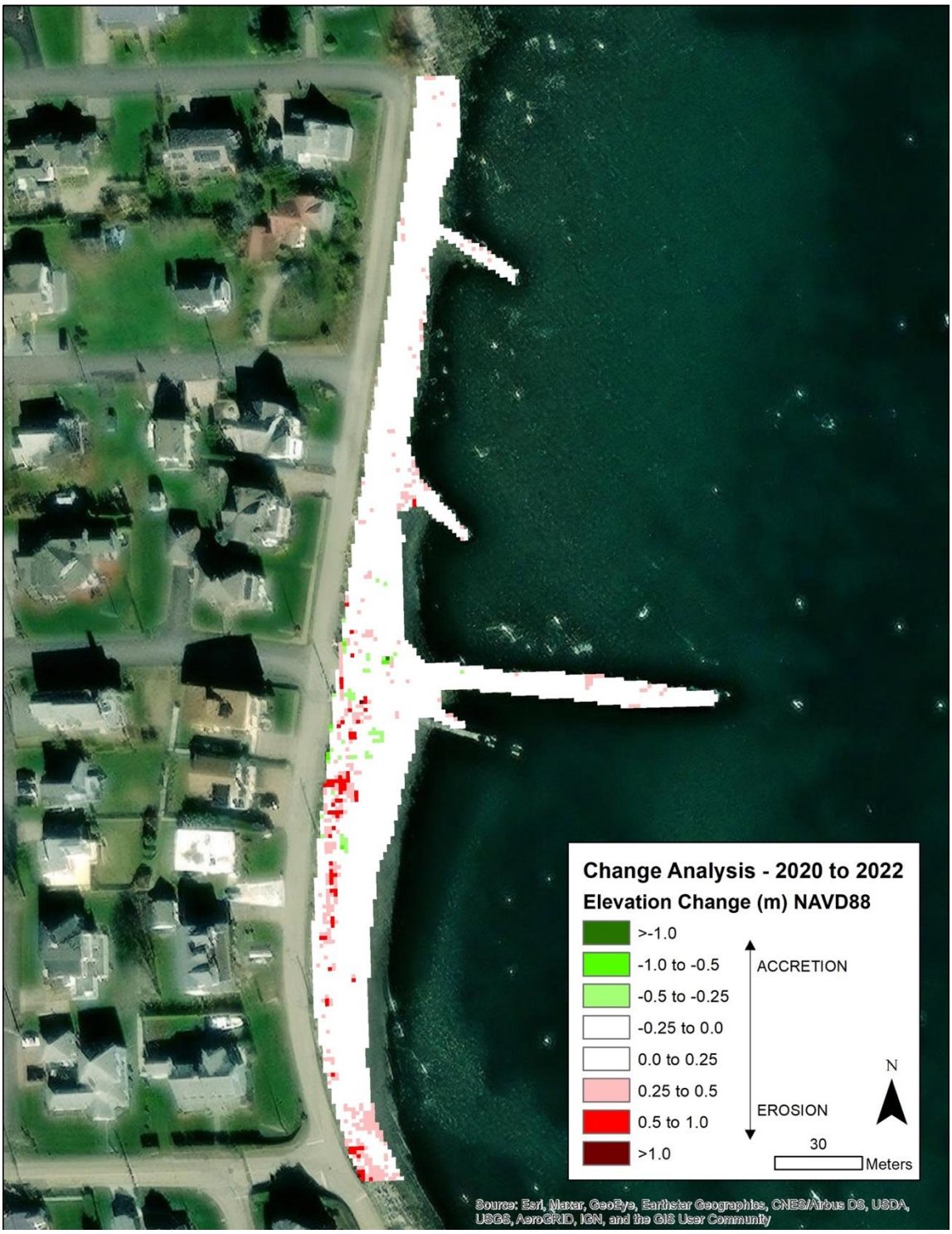

Figure 2-10. Change analysis September 9, 2020 to October 19, 2022.
Elevation change analysis created from DEMs generated from boat-based LiDAR scans collected on September 9, 2020 and October 19, 2022. Green colors indicate accretion and red colors indicate erosion.

2.4 Conclusions

New boat-based LiDAR scans were collected along Little Beach on September 9, 2020 and October 19, 2022. The raw LiDAR data were parsed with high precision position and orientation data, generating georeferenced point clouds. These point clouds were processed to eliminate irrelevant points, leaving only bare-earth points representing elevations along the beach. The resulting point clouds were then gridded to 1x1 meter Digital Elevation Models (DEMs). Volumes of Little Beach sediment were calculated as 6,164 cubic meters (above NAVD88) and 5,781 cubic meters (above NAVD88) for the September 2020 and October 2022 surveys, respectively. A change analysis map was produced, comparing the differences in elevation between the September 2020 and October 2022 surveys. Beach volume decreased slightly in the two years between the surveys (-6.2%).

Two surveys are insufficient to define a trend but we have been doing an identical LiDAR- monitoring program at Narragansett Town Beach (NTB) between 2019-2024 and have observed a trend of slowly decreasing beach volumes at that location over that longer interval. That decreasing trend has occurred at NTB despite sporadic efforts to replenish NTB with sand derived from inland sources. We have interpreted the trend observed at NTB as due to the combined effects of sea level rise and possibly increasing storm intensity. Similar processes are likely to be operating at Little Beach.

The data obtained from the two LiDAR surveys of Little Beach are sufficient to use for damage assessments in case the Little Beach area experiences a large storm event during the near future.

It is noteworthy that the largest losses in beach volume are occurring in front of the stone revetment that protects the road just landward of Little Beach. Similar losses are typically observed on beaches backed by hard structures. These structures tend to deflect wave energy downward in front of the structure during storms and the deflected wave energy tends to scoop up sand from the beach and carry it offshore (Van Rijn, 1998)

2.5 References

Baron, H.M., Kaminsky, G.M. 2012. Multibeam echosounder and mobile laser scanning data report for coastal and marine spatial planning Olympic Coast, Wahkiakum County, and mouth of the Columbia River. Unpublished Technical Report. 1-33.

Caccioppoli, B.J., King, J.W., Oakley, B.A., 2017a. Establishing protocols for monitoring bluff erosion using mobile terrestrial laser scanning from study sites along the Rhode Island coastline. *Unpublished technical report*.

Caccioppoli, B.J., King, J.W., Bartley, M.L., Davis, S.M., 2017b. Comparing topo-bathymetric surfaces and elevation transects along southern Rhode Island beaches. *Coastal Estuarine Research Federation Conference*, Providence, RI. November 9, 2017.

Davis, R.A., Fox, W.T., Hayes, M.O. and Boothroyd, J.C., 1972. Comparison of ridge and runnel systems in tidal and non-tidal environments. *Journal of Sedimentary Petrology*. (2). 413-421.

Hayes, M.O. and Boothroyd, J.C., 1969. Storms as modifying agents in the coastal environment. Coastal Research Group, Coastal Environments NE Massachusetts and New Hampshire. Univ. Massachusetts Dep. Geol., Amherst, Mass., 245-265.

Kaminsky, G.M., Baron, H.M., Hacking, A., McCandless, D. 2014. Mapping and monitoring bluff erosion with boat-based lidar and the development of a sediment budget and erosion model for the Elwha and Dungeness littoral cells, Clallam County, Washington. *Unpublished Technical Report.* 1-44.

Lacey, E.M. and Peck, J.A., 1988. Long-term beach profile variations along the south shore of Rhode Island, U.S.A. *Journal of Coastal Research*. 14(4). 1255-1264.

Van Rijn, L.C., 1998. Principals of Coastal Morphology. Aqua Publications, The Netherlands (WWW.AQUAPUBLICATIONS.NL)

3 Benthic Geologic Habitats of the Bonnet Shores Shoreface, Narragansett, Rhode Island

Authors: Bryan A. Oakley, Brian Caccioppoli, and John W. King

3.1 Introduction

This section summarizes efforts to map a portion of the shoreface offshore of Bonnet Shores, Narragansett, Rhode Island (Figure 3-1) using side-scan sonar data collected in July 2023 along with surface sediment grab samples and underwater video imagery collected in December 2023. Side-scan records are interpreted based on the texture and intensity of the returning acoustic signal (backscatter). Spatially distinct areas exhibiting different backscatter patterns represent side-scan sonar facies, which are specific seafloor areas delineated by the pattern, strength, and texture of the returning sonar signal; typically, the denser the bottom, the stronger the return signal, resulting in darker side-scan sonar records (utilizing an inverse color scheme). These delineated polygons, supplemented with underwater video imagery, aerial imagery, bathymetry, surficial sediment samples, sediment-profile images, and/or sediment core data, are interpreted to identify benthic geologic habitats. Seafloor habitats are identifiable spatial regions with physical, chemical, and/or biological attributes that differ from their surroundings (Greene et al., 1999). A benthic geologic habitat or depositional environment is a distinct spatial area with geologic characteristics that notably differ from neighboring regions (Oakley et al., 2012). The benthic geologic habitats in the study area were categorized using the Substrate Component (describing sediment grainsize) within the Coastal Marine Ecosystem Classification Standard (CMECS) classification system (FGDC, 2012). Similar approaches have been used in other areas to map shallow seafloor habitats (e.g., LaFrance Bartley et al., 2022; Oakley et al., 2012; Ozmon et al., 2017). Overlays were created to add additional information regarding biologic characteristics of the area, notably the presence of eelgrass (*Zostera marina)* and slipper shells (*Crepidula fornicata).*

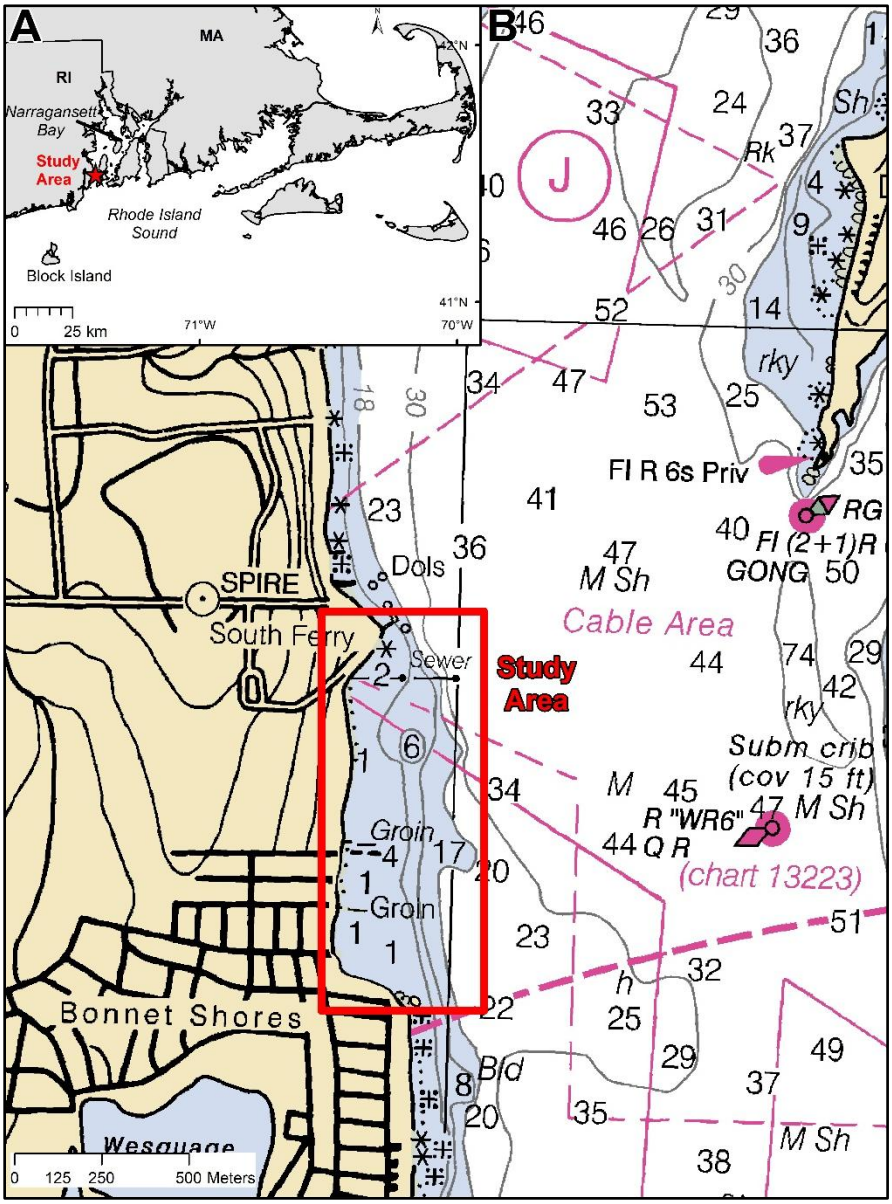

Figure 3-1.
(A) Location of the study area in southwestern Narragansett Bay.
(B) NOAA Chart 13221 showing the extent of the study area between the Graduate School of Oceanography at South Ferry Rd and the Bonnet Shores bedrock headland to the south.

3.2 Methods

Geophysical Data Collection

Side-scan sonar field methods

Geophysical investigations were undertaken using a bow-mounted EdgeTech 6205 Multi-Phase Echo Sounder system featuring dual-frequency side-scan (550 kHz and 1600 kHz), which simultaneously captures co-located side-scan and bathymetry data and is tailored for shallow water surveying, thereby enhancing survey efficiency. The survey was preplanned in Hypack (hydrographic surveying software) and devised to gather full-coverage side-scan data (i.e., achieving 100% coverage with 20-30% overlap). The survey consisted of parallel track lines with line spacing ranging from 35 m - 40 m (115 ft - 130 ft) and a sonar swath range of 50 m (165 ft) to ensure adequate overlap with neighboring lines. Additional survey lines parallel to the shoreline were adjusted on the fly to accommodate areas deemed unnavigable.

Side-scan Sonar Data Processing

Geophysical data was retrieved at the end of the field day. Each sonar file was exported individually from the Ocean Imaging Consultants GeoDAS sonar data acquisition software as Extensible Triton Format (*.XTF) files following the conclusion of the fieldwork. Subsequently, the *.XTF files were imported into Chesapeake Technologies SonarWiz Software (v. 6.0). The subsequent general processing sequence was executed for the files within the dataset. Navigation check on each file (including offset and layback applied), smoothing and editing if necessary.

- Bottom tracking of each individual sonar file
- Application of gain curves to normalize the data across the full sweep range and over the duration of the field program.
- Draft mosaic generated to check gain settings, bottom tracking, image quality and resolution.
- Manual editing of applied functions if necessary.
- Export of the sonar mosaic in format suitable for graphics software.
- For this project, a geo-referenced TIF image was exported out of SonarWiz for import and presentation in ArcMap GIS software (ESRI). Individual sonar files were also exported as geotif images to aid interpretation of the seafloor.

Navigation and Positioning Systems

An Applanix POS MV (V4) Inertial Navigation System, a high-precision position and orientation system blending satellite GPS data with angular rate and acceleration from an Inertial Measurement Unit (IMU) and Hypack V2015 navigation software were employed to precisely determine the vessel and geophysical sensors' locations throughout the data collection initiative. The manufacturer indicates a position accuracy between 0.2 to 2 meters under normal operating conditions. The dual GPS antennas within this system also offer heading information and can produce certain motion parameters, contingent upon the antenna configuration aboard the vessel; roll measurements are obtained when the antennas are aligned side-to-side (as in this survey), while pitch values are outputted when antennas are mounted along the vessel centerline fore to aft. This system boasts heading accuracies of 0.02° with update rates for all measurements of up to 200 Hz.

Ground-truth Information

The ground-truth survey encompassed the gathering of benthic grab samples from the seafloor using a Wildco Petite Ponar grab sampler in conjunction with underwater video imagery. Images at the surface sediment sample stations were captured by a GoPro video camera mounted above the sampler enabling co-located sediment samples/video imagery datasets (

Figure 3-2). The positions of the samples were logged using a Garmin GPSMAP76 handheld chart plotting GPS. Video drifts were also conducted using a custom-built PVC sled that drifts two GoPro cameras recording the seafloor at oblique and plan views (

Figure 3-3: Custom built PVC Camera sled used to record underwater video imagery along the drift shown in

Figure 3-6.

). The starting and ending positions of each drift was recorded. When combined with the geophysical data, these datasets contribute to a comprehensive understanding of the shoreface, capturing sediment characteristics and biological community characteristics across various spatial scales and resolutions. Underwater videos required minimal processing. Videos were trimmed to remove extraneous footage at the beginning and end of the videos, and title sides and end credits were added. The videos were exported as 1080 DPI HD *.mp4 videos. The *.mp4 files were then uploaded to YouTube for ease of sharing.

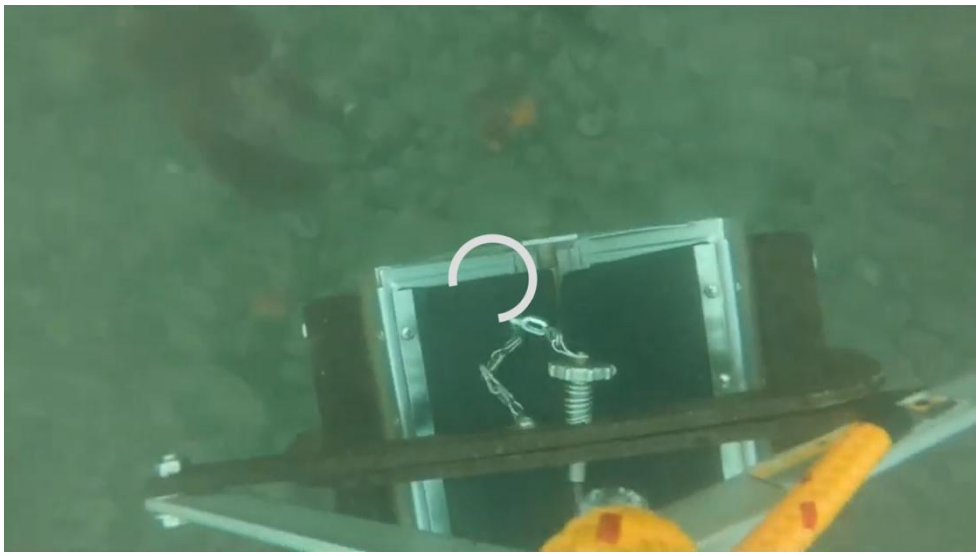

Figure 3-2: View of the Wildco Petite Ponar sediment sampler recorded from a GoPro camera mounted just above the sediment sampler.
Image collected from the video recorded at Bonnet Sample 19. See Figure 3-5 for the location of samples.

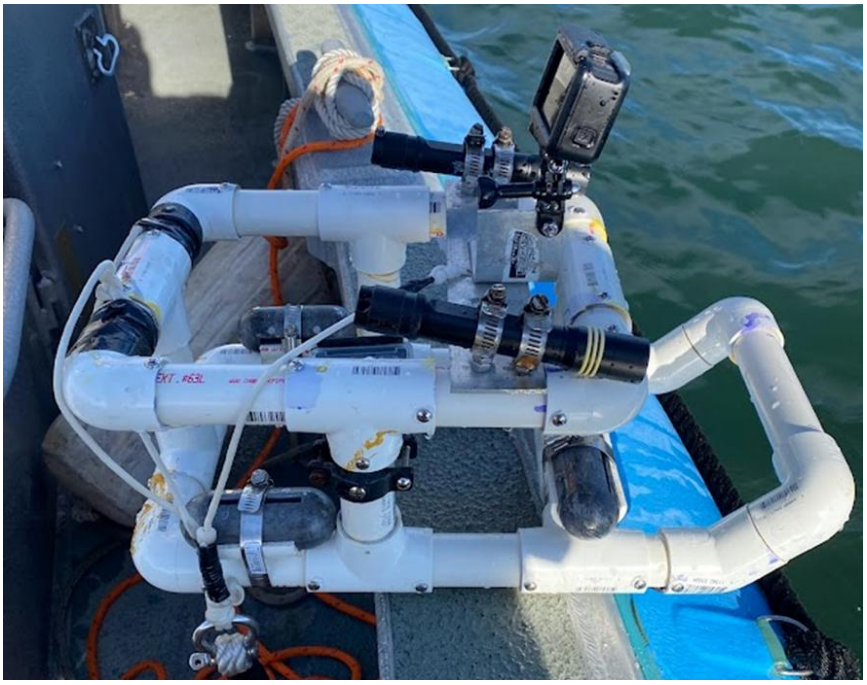

Figure 3-3: Custom built PVC Camera sled used to record underwater video imagery along the drift shown in

Figure 3-6.

3.3 Results

Side-scan sonar

A total of 281,000 m^2 (69 acres) of the shoreface offshore of Bonnet Shores was mapped with full-coverage side-scan sonar (See Figure 3-4 for the extent of side-scan coverage). Data was collected to the navigable limit of the survey vessel. The sonar data is displayed using an inverse Klein color scale, a yellow-brown color ramp where harder, generally coarser-grained and rougher seafloor habitats produce a stronger (darker) side-scan sonar return.

Figure 3-4. Digital side-scan sonar mosaic collected in July 2023 offshore of Bonnet Shores, Rhode Island.

Surface sediment grab samples

Surface sediment samples were collected at 21 locations within the mapped area. Figure 3-5 shows the location of the sediment samples collected. The spatial location, water depth and field notes are summarized in Table 3-1. The grainsize of selected sediment samples determined using the Malvern Mastersizer are reported in table 2. The grainsize of the samples ranged from 70 to 96% sand and were mostly 'Sand' in the Shepard (1954) classification scheme. Several samples contained abundant shell hash, as noted in the field descriptions, but these particles were too large to be analyzed in the Mastersizer, which has a maximum grainsize of 1 mm.

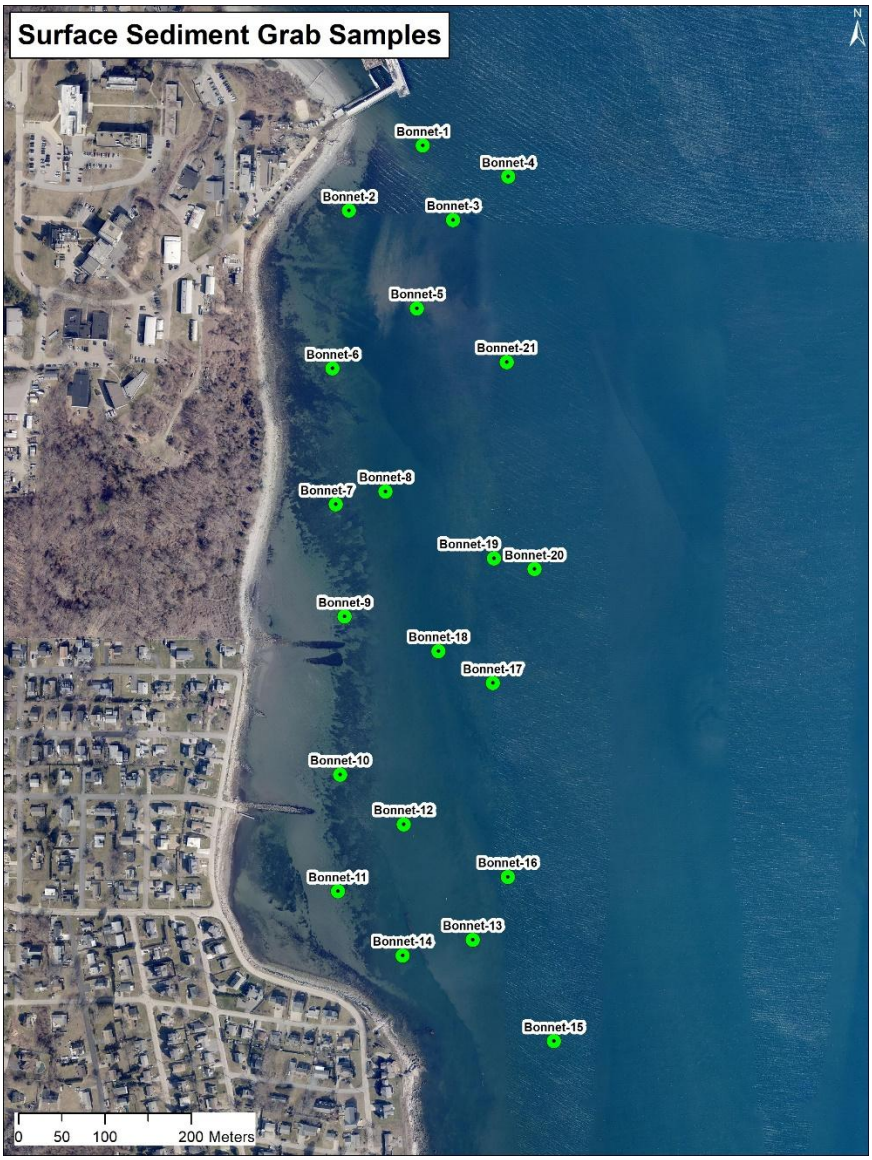

Figure 3-5. Location of surface sediment samples and underwater video imagery collected on 14 December 2023.

Table 3-1: Surface sediment grab samples collected offshore of Bonnett Shores on 14 December 2023.

Sample	Lat DD	Long DD	Depth (m)	Field Description
Bonnet-1	41.49163°	-71.41828°	8.2	*Crepidula*, oyster shells, trace of mud
Bonnet-2	41.49093°	-71.41928°	2.4	Cobble, some sand and pebbles and eelgrass
Bonnet-3	41.49086°	-71.41783°	3.8	Pebbly gravel, *crepidula* and macroalgae
Bonnet-4	41.4913°	-71.4171°	12.8	Silty fine sand abundant shell hash to gravel size; deep hole
Bonnet-5	41.48993°	-71.4183°	3.9	Macroalgae and *crepidula*
Bonnet-6	41.48928°	-71.41945°	2.9	Fine sand, trace of silt, shell fragments and eelgrass
Bonnet-7	41.48786°	-71.41935°	2.4	Fine sand, trace of silt, shell fragments and eelgrass
Bonnet-8	41.48801°	-71.41866°	3.2	Silty fine sand, shell fragments and eelgrass
Bonnet-9	41.4867°	-71.41918°	2.1	Fine sand, trace of silt, shell fragments and eelgrass
Bonnet-10	41.48505°	-71.41918°	2.3	Fine sand, trace of silt, shell fragments and eelgrass
Bonnet-11	41.48383°	-71.41916°	1.8	Fine sand, shell hash and eelgrass
Bonnet-12	41.48455°	-71.41828°	3.6	Fine sand, some silt, shell hash
Bonnet-13	41.48336°	-71.41728°	5.8	Fine sand, trace of silt, shell hash
Bonnet-14	41.48318°	-71.41825°	3.0	Fine sand, trace of silt shell hash; 1cm quahog
Bonnet-15	41.48233°	-71.41611°	8.2	Medium sand, some gravel abundant shell hash and mussel shells
Bonnet-16	41.48403°	-71.41681°	7.2	Silty cohesive sand with abundant shell fragment, trace gravel
Bonnet-17	41.48605°	-71.41718°	7.0	Cohesive sand, some silt, some pebble, shell fragments and *crepidula*
Bonnet-18	41.48636°	-71.41786°	4.7	Fine sand, trace of silt, shell fragments
Bonnet-19	41.48735°	-71.41713°	5.5	Silt, some sand and *crepidula*
Bonnet-20	41.48725°	-71.41656°	7.2	Shell hash, *crepidula* some sand and mussel shells
Bonnet-21	41.48940°	-71.41703°	5.5	*Crepidula*, red macroalgae

Table 3-2: Grainsize of the nine surface sediment samples analyzed. Grainsize classified using the Shepard (1954) classification scheme.

Sample	Percent Clay	Percent Silt	Percent V. Fine Sand	Percent Fine Sand	Percent Medium Sand	Percent Coarse Sand	Total Percent Sand	Shepard Class
Bonnet 6	0.2	3.7	8.0	39.8	32.3	15.9	96.1	Sand
Bonnet 7	0.3	7.8	6.9	36.2	40.3	8.7	92.0	Sand
Bonnet 8	2.6	26.5	16.4	30.9	20.4	3.2	71.0	Silty Sand
Bonnet 9	0.1	5.8	12.2	50.3	31.3	0.3	94.0	Sand
Bonnet 10	0.0	3.7	8.0	39.8	32.3	15.9	96.1	Sand
Bonnet 11	0.3	3.5	6.4	48.1	37.9	3.9	96.3	Sand
Bonnet 12	0.6	13.1	17.0	43.9	25.1	0.3	86.4	Sand
Bonnet 13	1.3	12.5	7.8	37.9	35.2	5.3	86.2	Sand
Bonnet 14	0.2	6.5	13.5	47.3	31.5	1.0	93.3	Sand

Underwater video imagery

Underwater video imagery was collected at 20 of the surface sediment grab stations; one video was omitted due to a camera failure at station 2. Additionally, 11 video drifts (

Figure 3-6) were recorded to examine the transitions between side-scan sonar facies. Full videos can be found at YouTube links provided in tables 3-3 and 3-4.

Figure 3-6. Underwater video drifts collected on 14 December 2023.
All videos were collected drifting from north to south along the lines shown.

Table 3-3: Underwater video images collected at the surface sediment grab sample locations.

Sample	Lat DD	Long DD	Depth (m)	YouTube Link
Bonnet-1	41.49163°	-71.41828°	8.2	https://youtu.be/hTLSXny3HMY
Bonnet-2	41.49093°	-71.41928°	2.4	https://youtu.be/j1sRiBRJsCE
Bonnet-3	41.49086°	-71.41783°	3.8	https://youtu.be/bCQHEcRbtdI
Bonnet-4	41.4913°	-71.4171°	12.8	https://youtu.be/6OJKBT4yTx4
Bonnet-5	41.48993°	-71.4183°	3.9	https://youtu.be/Aip1oDizfbs
Bonnet-6	41.48928°	-71.41945°	2.9	https://youtu.be/CroXhv4xpsk
Bonnet-7	41.48786°	-71.41935°	2.4	https://youtu.be/oEiUNQlZ9HQ
Bonnet-8	41.48801°	-71.41866°	3.2	https://youtu.be/2tmFOj7ckvI
Bonnet-9	41.4867°	-71.41918°	2.1	https://youtu.be/Qbgzf02a9xM
Bonnet-10	41.48505°	-71.41918°	2.3	https://youtu.be/SyObtoS3bQc
Bonnet-11	41.48383°	-71.41916°	1.8	https://youtu.be/8Ayz7LctEHM
Bonnet-12	41.48455°	-71.41828°	3.6	https://youtu.be/yoAdw_5oFyc
Bonnet-13	41.48336°	-71.41728°	5.8	https://youtu.be/1zsmwlAdKjY
Bonnet-14	41.48318°	-71.41825°	3.0	https://youtu.be/yejn5JMw0RA
Bonnet-15	41.48233°	-71.41611°	8.2	https://youtu.be/MxEaD3o5pzM
Bonnet-16	41.48403°	-71.41681°	7.2	https://youtu.be/5fO_R-c1P6Y
Bonnet-17	41.48605°	-71.41718°	7.0	https://youtu.be/dJzg4jT7xbM
Bonnet-18	41.48636°	-71.41786°	4.7	https://youtu.be/9c3XAe-3UX4
Bonnet-19	41.48735°	-71.41713°	5.5	https://youtu.be/ieXDKqWMECg
Bonnet-20	41.48725°	-71.41656°	7.2	https://youtu.be/2AR8ocvWXZ8
Bonnet-21	41.48940°	-71.41703°	5.5	https://youtu.be/OdAMdPS1SwU

Table 3-4: Underwater video drifts collected along 11 lines within the study area. See provided figure for the location. All drifts went from north to south, beginning and ending at the points noted. Water depth was recorded at the start of each line.

Drift Point	Lat DD	Long DD	Depth (m)	YouTube Link
Drift 1 Start	41.48932	-71.41920	2.4	https://youtu.be/k9AHLGnpxnE
Drift 1 End	41.48878	-71.41917		
Drift 2 Start	41.48780	-71.41945	1.6	https://youtu.be/mWp5IsA-MLE
Drift 2 End	41.48752	-71.41942		
Drift 3 Start	41.48663	-71.41915	1.4	https://youtu.be/jGR31EmpO2w
Drift 3 End	41.48627	-71.41892		
Drift 4 Start	41.48508	-71.41915	1.9	https://youtu.be/2e6QlXAcS4U
Drift 4 End	41.48497	-71.41903		
Drift 5 Start	41.48637	-71.41760	5.2	https://youtu.be/9hYgceQJ9cQ
Drift 5 End	41.48600	-71.41735		
Drift 6 Start	41.48525	-71.41762	5.2	https://youtu.be/phwMuEtvtcI
Drift 6 End	41.48442	-71.41723		
Drift 7 Start	41.48755	-71.41892	2.0	https://youtu.be/xCJp3DrKLxo
Drift 7 End	41.48733	-71.41877		
Drift 8 Start	41.48830	-71.41778	4.3	https://youtu.be/_u_VPNnJ51o
Drift 8 End	41.48792	-71.41762		
Drift 9 Start	41.48750	-71.41670	7.0	https://youtu.be/gBBbfPn7IZg
Drift 9 End	41.48678	-71.41653		
Drift 10 Start	41.49075	-71.41847	2.3	https://youtu.be/RCAE9ZIZWyk
Drift 10 End	41.49032	-71.41830		
Drift 11 Start	41.49030	-71.41903	2.3	https://youtu.be/aFsA2FUKEXE
Drift 11 End	41.49013	-71.41893		

Surface sediment characteristics

The surface sediment characteristics of the study area were classified using the Substrate Component within the CMECS classification system (FGDC, 2012). The sediment generally grades from sandy or gravelly sediment along the shoreline/uppermost shoreface to silty sand and gravelly muddy sand further offshore (Figure 3-7). Within the mapped study area, fine sand (62%) and Silty Sand (22%) are the two dominate substrates. One exception to this trend are the areas of gravelly sand in the southern portion of the study area and on a bathymetry high in the center of the study area. Bedrock was mapped along the southern edge of the study area and extend onshore to subaerial bedrock outcrop. Boulders were mapped along the bedrock outcrops and where three shoreline protection structures (groins) extended into the study area. Table 3-5 summarizes the CMECS Classification of the mapped polygons.

Table 3-5:CMECS Substrate Classification of the Bonnet Shores study area.

CMECS Substrate Classification						
Origin	**Class**	**Subclass**	**Group**	**Subgroup**	**Area (Acres)**	**Area (m^2)**
Geologic	Rock Substrate	Bedrock	Bedrock	Bedrock	0.5	1,873
Geologic	Unconsolidated Mineral Substrate	Coarse Unconsolidated Substrate	Gravel	Boulder	0.9	3,576
Geologic	Unconsolidated Mineral Substrate	Fine Unconsolidated Substrate	Sand	Sand (Undif)	1.4	5,733
Geologic	Unconsolidated Mineral Substrate	Fine Unconsolidated Substrate	Sand	Fine Sand	42.9	173,689
Geologic	Unconsolidated Mineral Substrate	Fine Unconsolidated Substrate	Muddy Sand	Silty Sand	15.6	63,275
Geologic	Unconsolidated Mineral Substrate	Coarse Unconsolidated Substrate	Gravelly	Gravelly Sand	2.6	10,487
Geologic	Unconsolidated Mineral Substrate	Coarse Unconsolidated Substrate	Gravelly	Gravelly Muddy Sand	4.1	16,743
Geologic	Unconsolidated Mineral Substrate	Coarse Unconsolidated Substrate	Gravel Mixes	Sandy Gravel	1.5	6,026

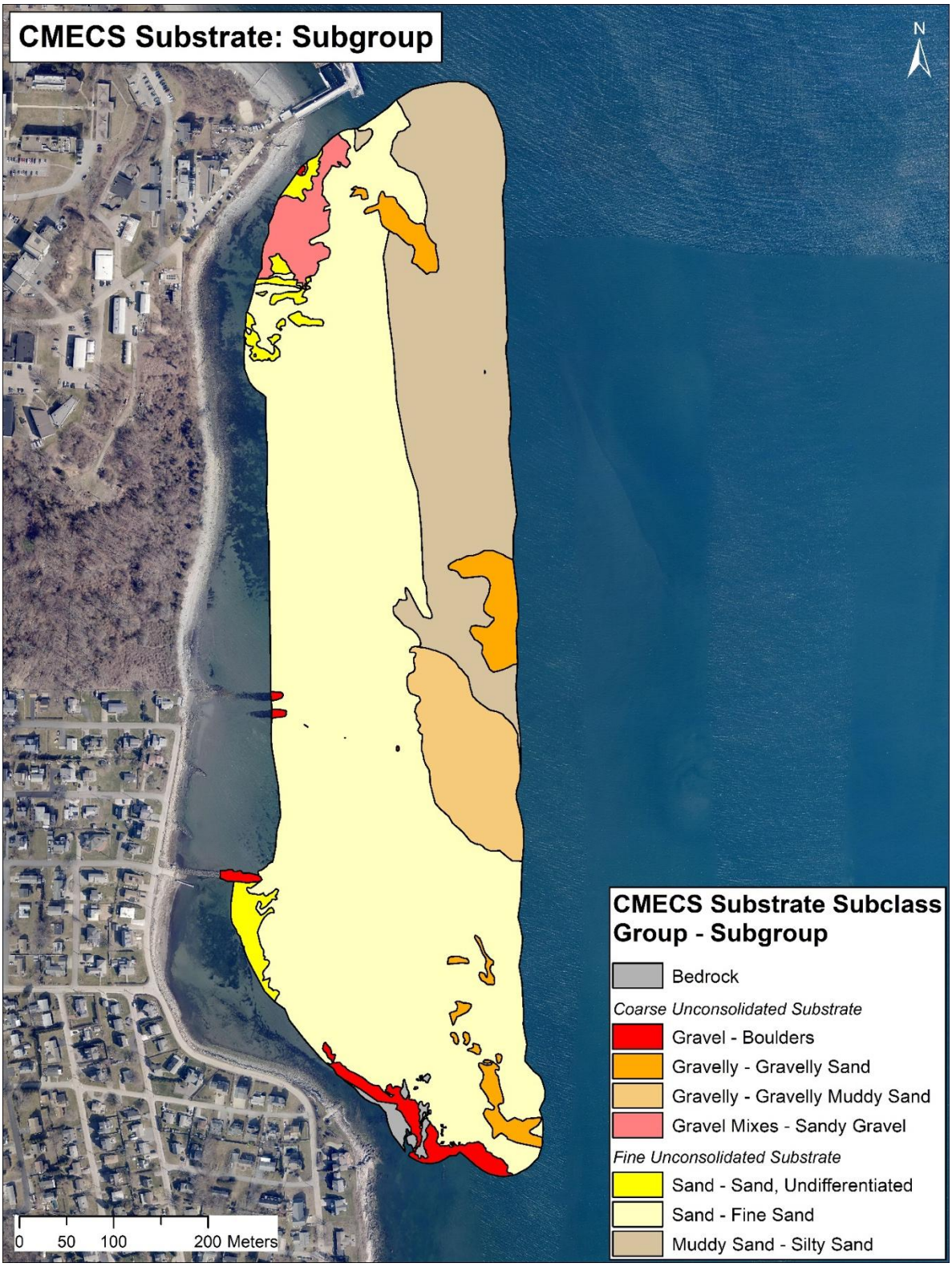

Figure 3-7. CMECS Substrate Component mapped offshore of Bonnet Shores to the Subgroup level.

Areas of dense Slipper Shells (*Crepidula fornicata)* were observed in the north/central portion of the study area. *Crepidula* Reef is a recognized biogenic substrate group within CMECS. Dense accumulations of these shells, both living organisms and shells/shell hash was common in both sediment samples and observed on underwater video imagery (**Error! Reference source not found.**). The relatively hard shells produced a slightly darker side-scan sonar return compared to areas of similar (mineral) substrate without dense accumulations of these shells.

Figure 3-8: Extent of dense Slipper Shells (Crepidula fornicata) mapped within the study area.

shows the extent of the dense accumulations of *Crepidula fornicate.* The extent of this was mapped independently of the geologic substrate, which was discerned from the sediment samples collected within these areas. The extent of the *Crepidula* reef is shown as an overlay on the geologic substrate in F

Figure 3-9) and was found across a range of sediment types.

Figure 3-8. Screen capture from the video collected along Drift 8, showing dense accumulation of Crepidula fornicata shells.

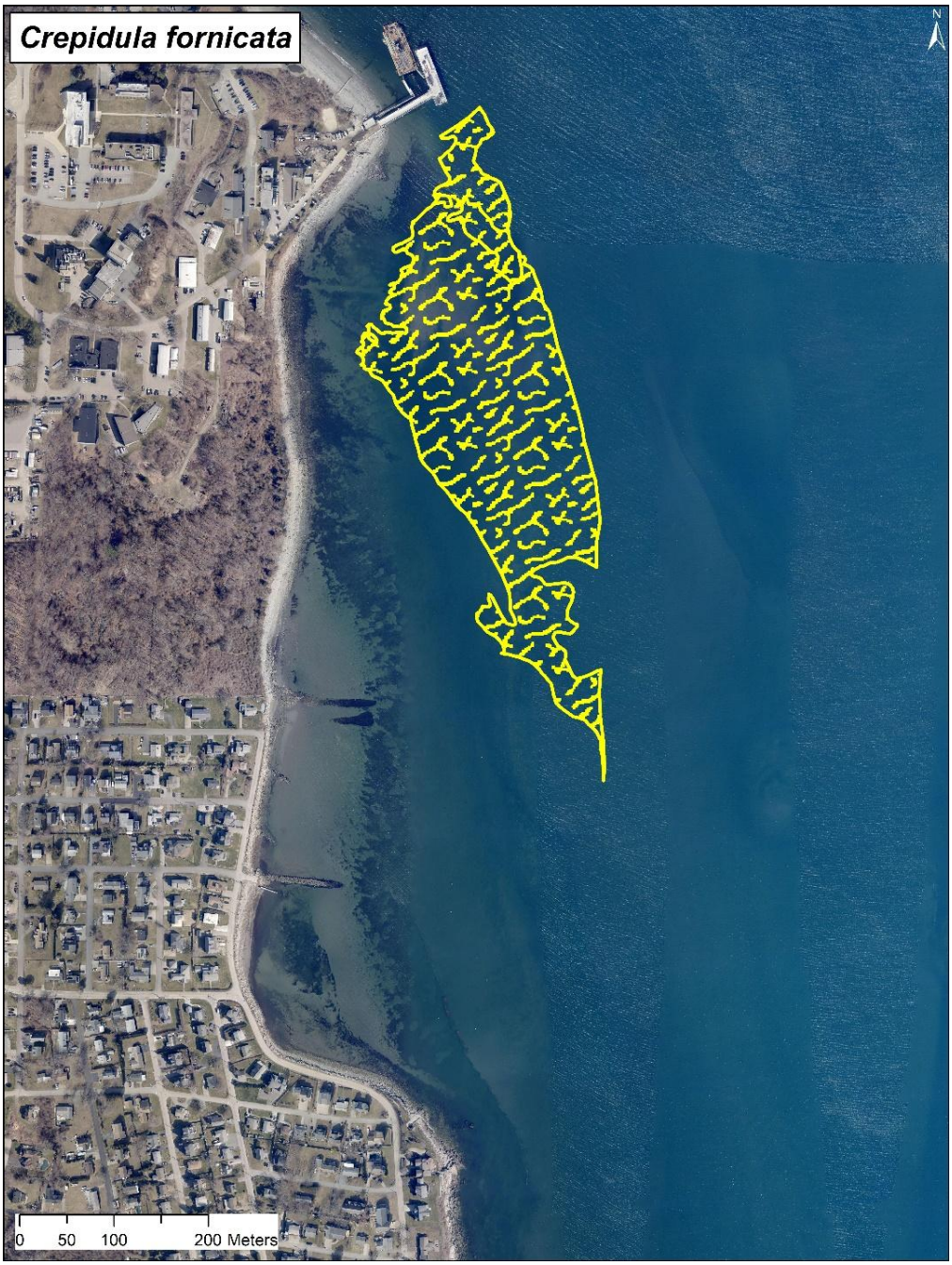

Figure 3-8: Extent of dense Slipper Shells (Crepidula fornicata) mapped within the study area.

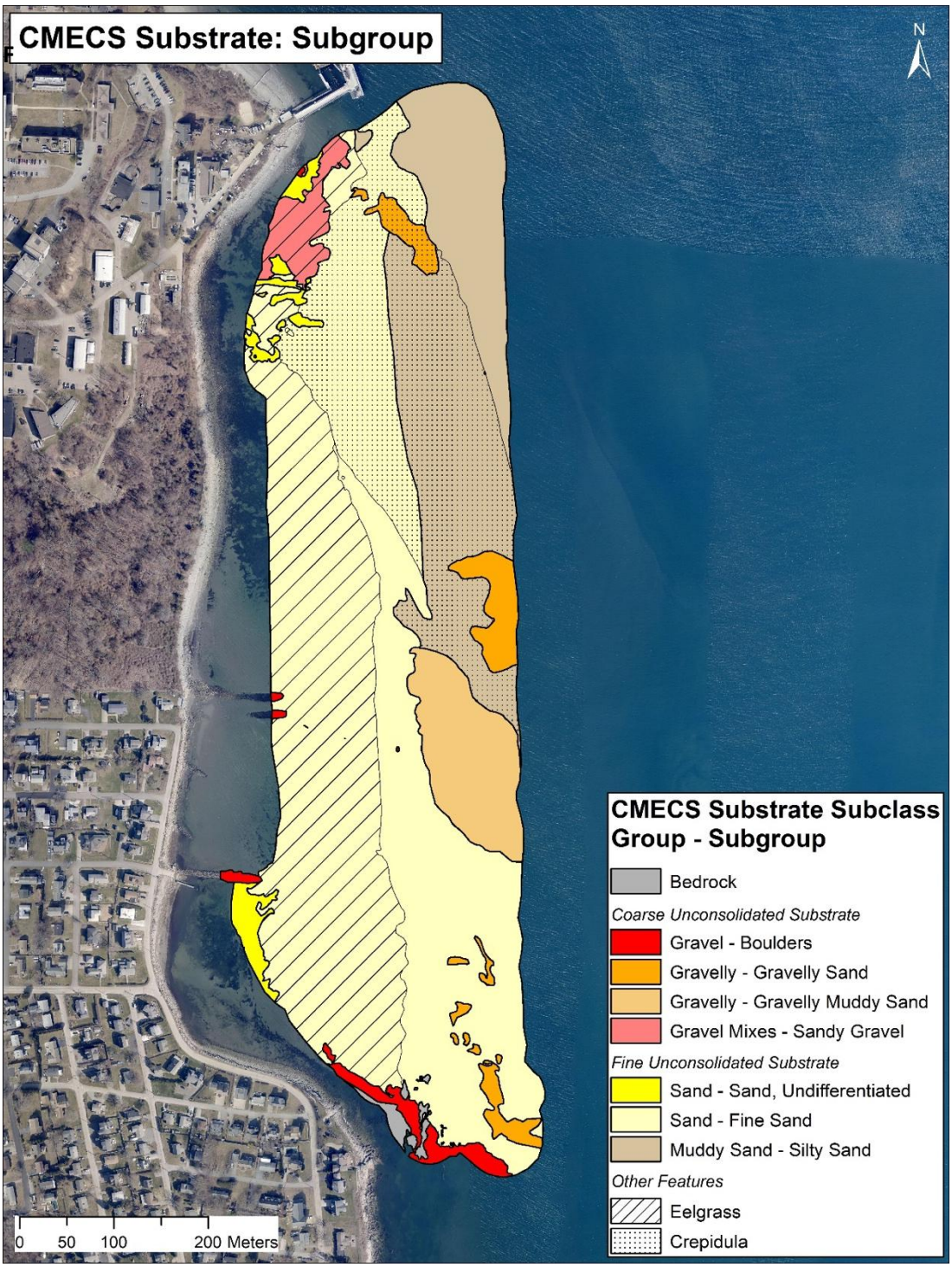

Figure 3-9. CMECS Substrate Component mapped offshore of Bonnet Shores to the Subgroup level showing the extent of Crepidula fornicate (stippled pattern) and eelgrass (hatched pattern).

Extent of eelgrass

The extent of eelgrass (*Zostera marina)* was delineated in two polygons, qualitatively differentiated based on the side-scan sonar return as 'dense' or 'scattered' eelgrass (Figure 3-10, Figure 3-11). Total mapped eelgrass coverage was 91,380 m^2 (22.6 acres), with 37,880 m^2 (9.4 acres) mapped as 'dense' and 53,500 m^2 (13.2 acres) mapped as 'scattered' (Figure 12). The extent of eelgrass is similar to the tier 1 aerial imagery conducted in 2021 (Bradley, 2023). The 2021 extent extends landward (shallower) than the 2023 mapping, so the total acreage of the eelgrass beds was not directly compared. The expansion of this eelgrass bed represents an area of increased eelgrass in the study area, in contrast to the broader regional decline in eelgrass beds elsewhere in Rhode Island (Bradley et al., 2022). The results of this study suggest that the eelgrass bed offshore of Bonnet Shores has persisted since 2021. This is an important finding, and future mapping (either aerial or using sonar) will help monitor the persistence of these eelgrass beds. Eelgrass is an essential habitat for organisms such as fish, epifauna, phytoplankton, and infauna, as well as a foraging habitat for migratory waterfowl (Leblanc, 2021). Eelgrass is designated as Essential Fish Habitat, (EFH), and is a Habitat of Particular Concern under the Magnuson-Stevens Fishery Conservation and Management Act in 1996, (NOAA, 2014). Additionally, Eelgrass is recognized as a critical marine resource and is by both federal and state regulations. Eelgrass beds are classified in CMECS under the Biotic Subclass of Aquatic Vascular Vegetation, and at the Biotic Group level, Seagrass Beds are recognized habitats. The extent of eelgrass is shown as an overlay on the interpreted substrate component in F

Figure 3-9.

The abundance of eelgrass found in the study area precludes the option of hydraulically dredging sand immediately offshore of Little Beach and depositing it onshore to replenish the beach. Dredging sand that infills the channel at the boat ramp would not be precluded, and this sand has been used in the past for replenishment. However the relatively low frequency of channel dredging and the limited volume of sand obtained would significantly mitigate ongoing coastal erosion at Little Beach.

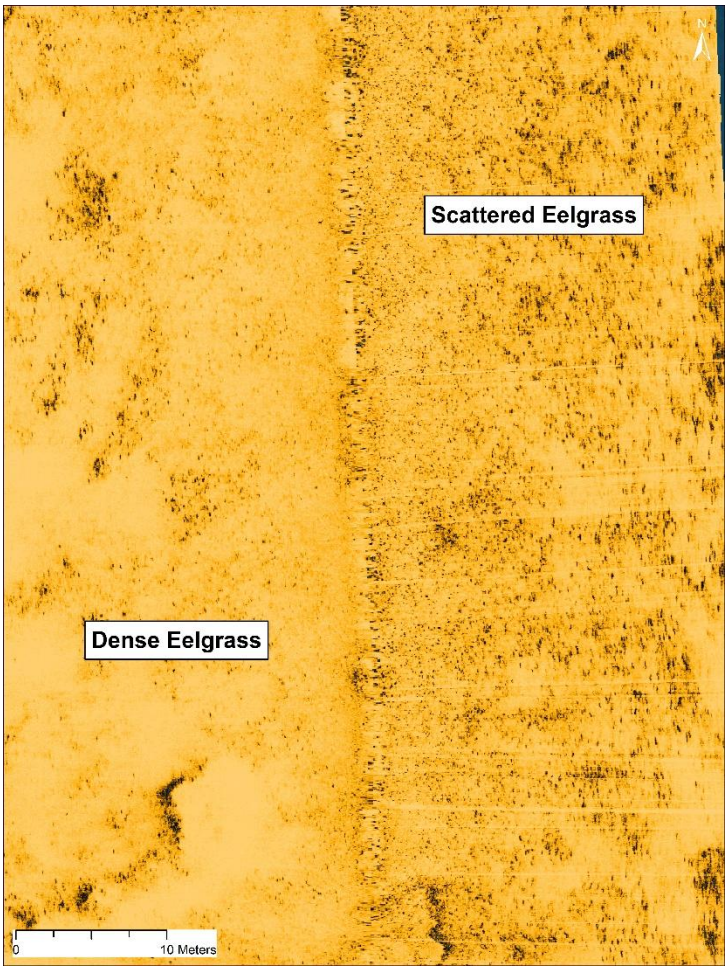

Figure 3-10. Portion of a side-scan sonar record showing an example of dense and scattered eelgrass mapped offshore of Bonnet Shores.
The very light areas on the left side of the image are the acoustic shadow produced by the eelgrass blades obscuring the sonar signal.

Figure 3-11. Screen capture from video drift 2 showing eelgrass shoots.

Figure 3-12: Extent of eelgrass beds mapped in this study (solid polygons) and 2021 (Bradley, 2023) red cross-hatched polygons.

3.4 References

Bradley, M., 2023, RI Submerged Aquatic Vegetation 2021 *in* Rhode Island Coastal Resources Management Council, U. E. D. C., Narragansett Bay National Estuarine Research Reserve ed.

Bradley, M., Boyd, J., Goetsch, B., Goulet, D., Mitchel, J., and LaBash, B., 2022, 2021 Tier 1 Mapping of Submerged Aquatic Vegetation (SAV) in Rhode Island and Change Analysis.

FGDC, 2012, Coastal and Marine Ecological Classification Standard (CMECS).

Greene, H. G., Yoklavich, M. M., Starr, R. M., O'Connell, V. M., Wakefield, W. W., Sullivan, D. E., McRea jr., J. E., and Cailliet, G. M., 1999, A classification scheme for deep seafloor habitats: Oceanologica acta, v. 22, p. 663-678.

LaFrance Bartley, M., King, J. W., Oakley, B. A., and Caccioppoli, B. J., 2022, Post-Hurricane Sandy Benthic Habitat Mapping at Fire Island National Seashore, New York, USA, Utilizing the Coastal and Marine Ecological Classification Standard (CMECS): Estuaries and Coasts, v. 45, no. 4, p. 1070-1094.

Leblanc, M.-L., 2021, Eelgrass (Zostera marina) ecosystems in eastern Canada and their importance to migratory waterfowl, McGill University (Canada).

Oakley, B. A., Alvarez, J. D., and Boothroyd, J. C., Benthic Geologic Habitats of Shallow Estuarine Environments: Greenwich Bay and Wickford Harbor, Narragansett Bay, Rhode Island, U.S.A2012.

Ozmon, I. M., Dobbs, K., Enterline, C., Dickson, S. M., and Nixon, M. E., Subtidal benthic habitat mapping with CMECS in mid-coast Maine *in* Proceedings Coastal and Estuarine Research Federation Biennial Conference Providence, RI, 2017, CERF.

4 Little Beach Area, Bonnet Shores, Narragansett, Rhode Island: Coastal Erosion Model

Authors: Reza Hashemi and Arash Rafiee Dehkharghani

4.1 Overview

The Little Beach area is situated within Bonnet Shores, along the coast of Narragansett Bay in Rhode Island, within the town of Narragansett (Figure 4-1). This area is vulnerable to coastal flooding and erosion because of a combination of factors, including powerful storms like hurricanes and Nor'easters, and rising sea levels. The interaction between rising sea levels and future coastal storms is expected to result in both increased flooding and erosion.

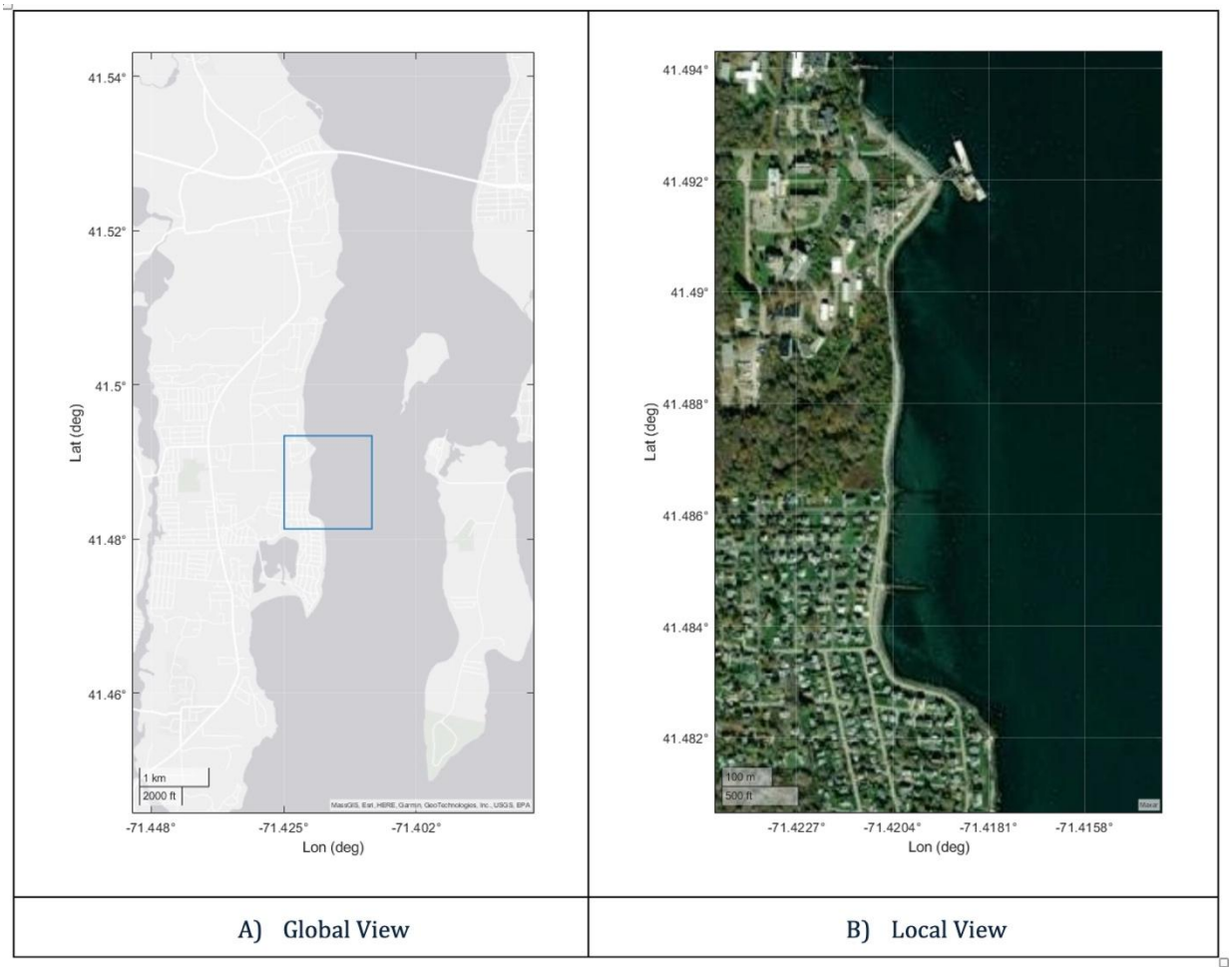

Figure 4-1. Location of Study Area

4.2 Objectives

The goal of this study is to investigate and assess the coastal erosion issues at the Little Beach area. Initiated by the Fire District, this effort seeks to comprehensively understand the mechanisms driving erosion and deposition in the study area while exploring viable conceptual engineering solutions for their mitigation in next steps.

This section of the report has the following specific objective:

- Predictive Modeling: Employ numerical modeling techniques to gain deeper insights into the underlying processes behind erosion and deposition within the study area, including wave and storm surge processes. The model will focus on the lower section of the west passage, spanning from Bonnet Point to the north of the URI Bay campus. The primary focus of this model will be the simulation of waves and coastal erosion dynamics, contributing to informed decision-making.
- Data collection for model validation.

4.3 Data

Field Measurement

To better understand the wave forcing in the Little Beach area, a wave buoy was deployed. The deployment location is shown in Figure 4-2. The wave height data collected from the buoy will also aid in model validation and assessment.

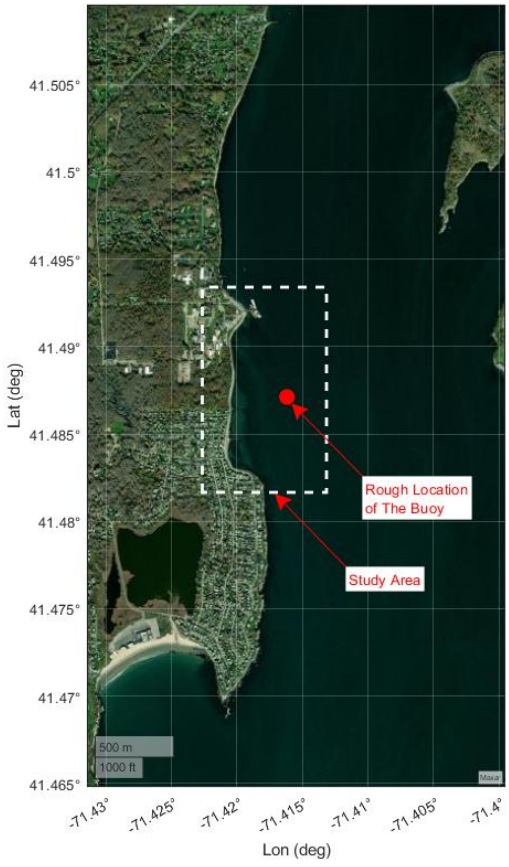

Figure 4-2. Location of The Deployed Buoy

Buoy – SOFAR SPOTTER

The SOFAR OCEAN Spotter buoy shown in Figure 4-3, is deployed to capture and analyze ocean wave data. This buoy measures wave frequencies ranging from very low (once every 30 seconds) to very high (once every second), with a precision of 2.5 measurements per second. It does not need any calibration. The Spotter records the movement of waves in three dimensions over time and internally processes this data to create a wave spectrum along with wave statistics such as significant wave height.

Top View

Front View

Figure 4-3. SOFAR Spotter Buoy

The data collected by the Spotter is stored within the device and can also be viewed through an online dashboard. In addition to wave analysis, the Spotter tracks and reports on a variety of other important marine conditions, including wind patterns and wave dynamics. It provides updates on the average and maximum wave period, and the speed and direction of the wind (the wind data is not as reliable as it is an estimate).

Deployment Process

The deployment process consisted of two phases. The first was the "Test Deployment" conducted at the Bay campus with coordinates 41.49409° N and 71.41930° W. The depth was approximately 7.5 meters, and the buoy was deployed directly from the beach using a small motorboat (Figure 4-4). This deployment lasted for just one day, from 06/06/2023 to 06/07/2023. The objective of this initial phase was to confirm the functionality of the buoy. During this time, the buoy was checked for stability, signal integrity, and other potential operational challenges. The results were satisfactory, indicating readiness of the buoy for a more extended deployment.

Figure 4-4. Small Motorboat Used for "Test Deployment."

Following this was the "Main Deployment" at Bonnet Shores with approximate coordinates 41.48729° N and 71.41641° W. The depth here was slightly deeper at approximately 8.2 meters, and the buoy was deployed using a Pontoon Boat. This phase commenced on 07/05/2023 and lasted for three months. The Pontoon Boat, and the different steps of Main Deployment are shown in Figure 4-5.

Pontoon boat used for “main deployment”

Prepration for the deployment

Deploying the buoy

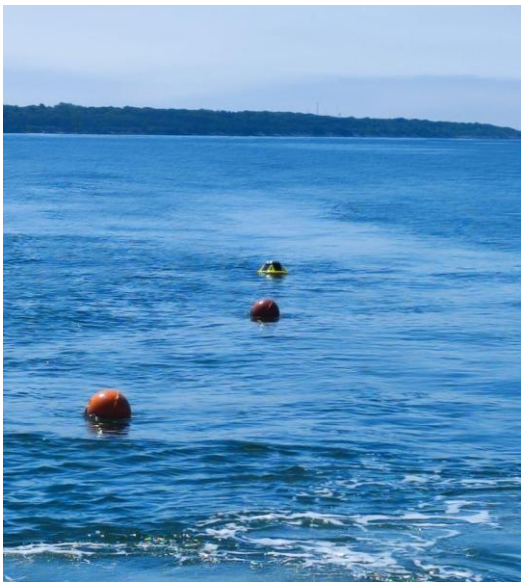

Deployed buoy with its surface sloats

Figure 4-5. Main Deployment

Data Analysis

In this section, the data reported in the online dashboard of wave buoy are shown. The significant wave height time series (Figure 4-7) and histogram (Figure 4-6), as well as the waverose of wave data (Figure 4-8) are provided. As these figures show, the average wave height during the deployment is around 0.25 m. There is also an event with wave height exceeding 2.7 m in the first week of October.

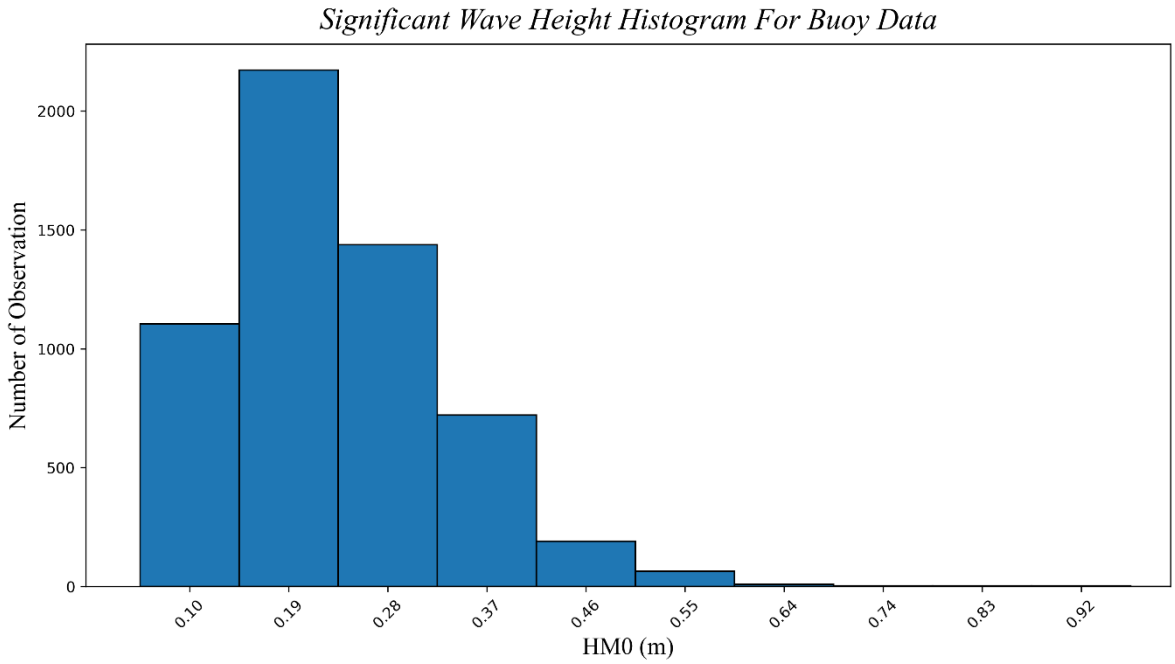

Figure 4-6. Significant Wave Height Histogram

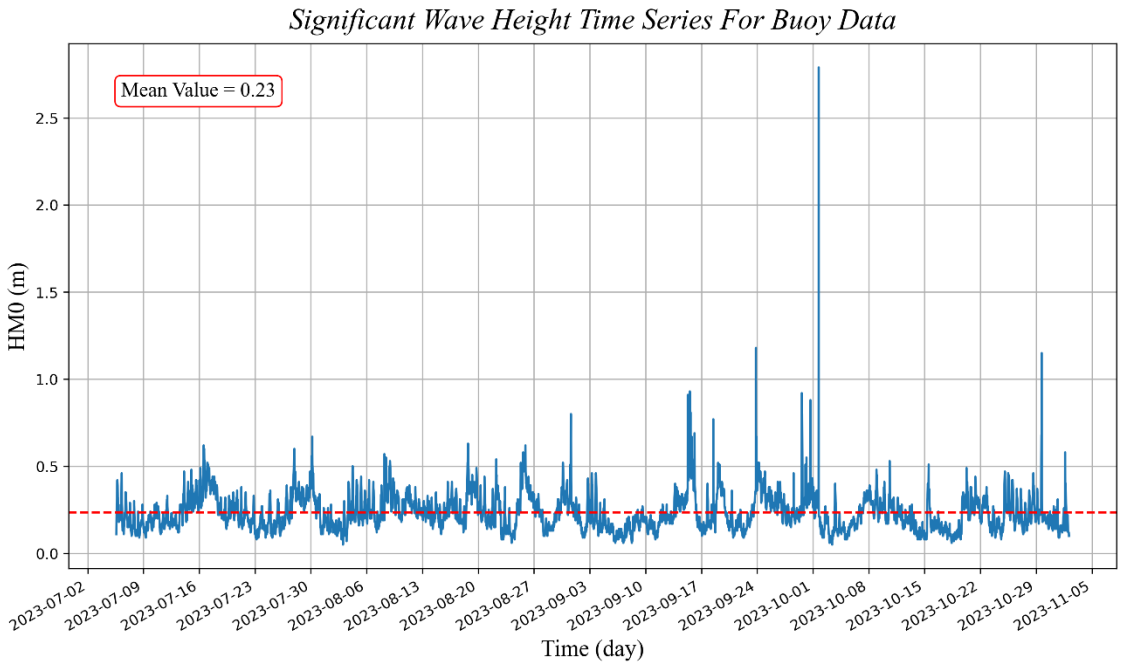

Figure 4-7. Significant Wave Height Time Series

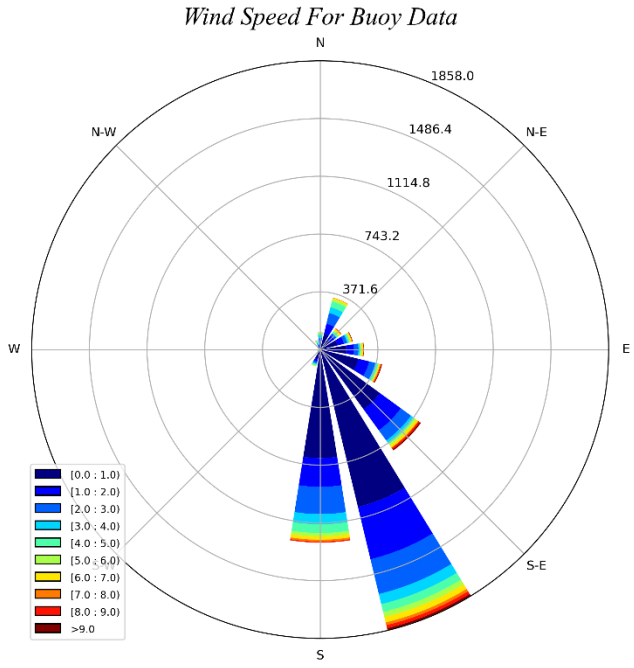

Figure 4-8. Waverose

Wind Data

To better understand the wind speed and direction variations at the site, wind data have been sourced from the National Data Buoy Center (NDBC) for stations within the Narragansett Bay. The NDBC stations are supported by the National Oceanic and Atmospheric Administration (NOAA). The wind datasets were gathered from 2005 to 2022 from Quonset Point and Newport stations. The specifications of these stations are summarized in the table.

Table 4-6 Specification of Stations

	New Port	**Quonset Point**
Station ID	NWPR1	QPTR1
Station Number	8452660	8454049
Coordination	41.504 N, 71.326 W	41.586 N, 71.407 W
Site elevation	2.2 m Above MSL[1]	1.6 m Above MSL
Air temp height	3.5 m Above SE[2]	4.4 m Above SE
Anemometer height	8.4 m Above SE	7.0 m Above SE
Barometer elevation	3.3 m Above MSL	3.1 m Above MSL
Sea temp depth	1.3 m below MLLW	6.1 m Below MLLW

Figure 4-9 shows the wind roses on average, as well as for summer and winter. As this figure illustrates, strong winds in summer typically come from the south and southwest, while in winter, the dominant winds originate from the north. The local wind pattern is particularly important during winter, as waves are generated in the bay by northerly winds.

[1] MSL: Mean Sea Level

[2] SE: Sea Level

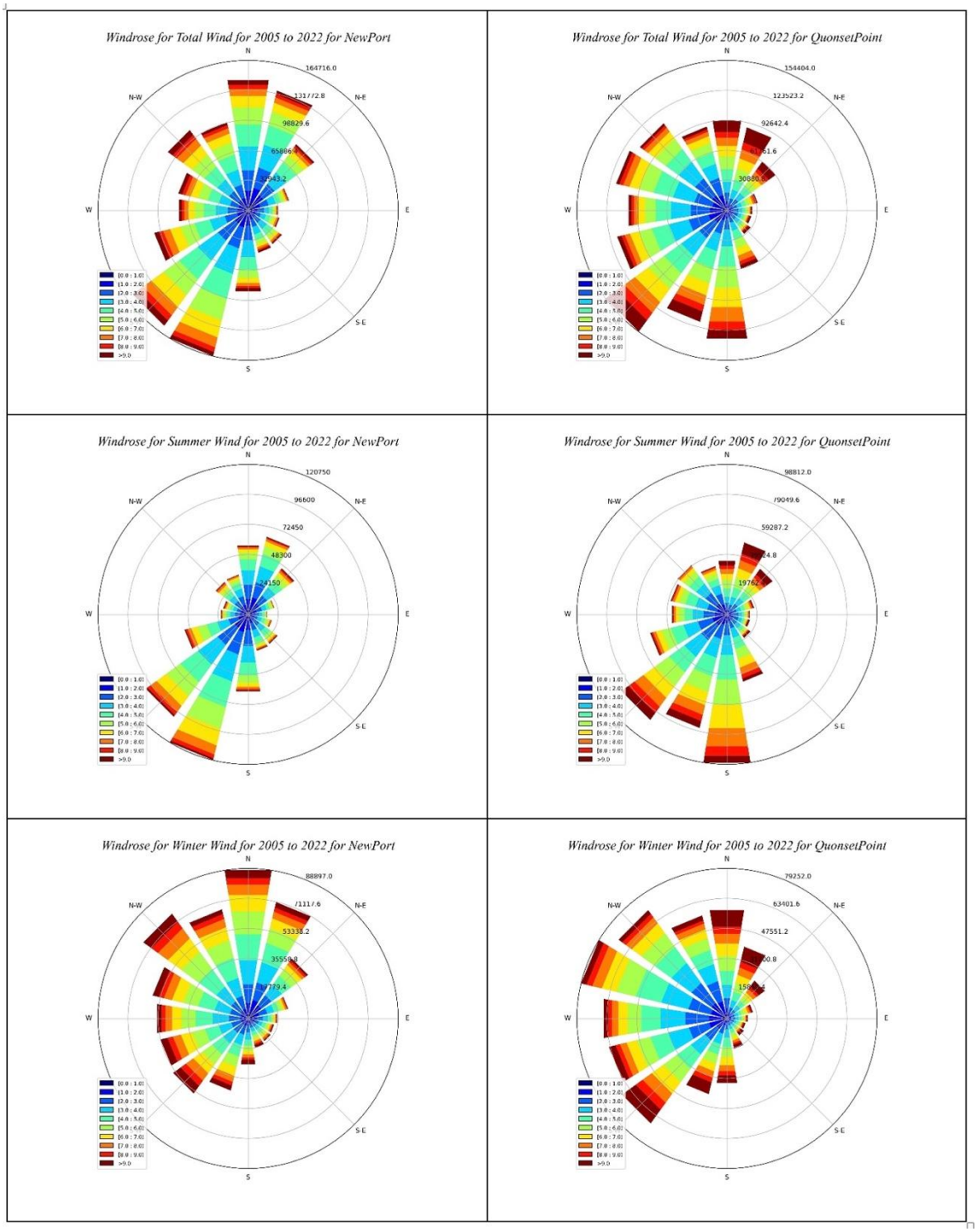

Figure 4-9. Seasonal Wind Rose Comparison.
Newport (Left) vs. Quonset Point (Right) - Annual, Summer, and Winter Patterns

4.4 Modeling

The SWAN[1] (Booij et al., 1999; Ris et al., 1999) model has been utilized alongside the measured data and WIS[2] dataset for wave modeling. For coastal morphology and sediment transport, the XBeach model (Roelvink et al., 2009) has been employed. The details of model development process are presented here.

SWAN Model

A stationary SWAN model is employed. In this mode, the peak wave height resulting from sustained wind speeds is estimated, and its propagation toward the coast is modeled.

Bathymetry

For model domain, the DEM Global Mosaic data is utilized for the initial modeling stage, as indicated in Figure 4-10. The bathymetry and topography data were originally generated in 2015 and subsequently updated on May 31, 2023. The area of interest coordinates is shown on Table 4-2. It should be noted for the purpose of the wave modeling, this data is sufficient while for coastal erosion assessments, more up to date data would be useful.

Table 4-2 Coordinates of the shaded area in Figure 4-13

North (Latitude)	+42.80°
South (Latitude)	+40.50°
East (Longitude)	-69.00°
West (Longitude)	-72.00°

[1] Simulating Waves Nearshore

[2] Wave Information Study

Figure 4-130. Geographical domain of the SWAN model

SWAN Model Setup

Based on the obtained bathymetry and topography dataset, the SWAN model is configured. The computational domain is visually represented in Figure 4-11. This domain spans from a longitude of -71.9 degrees west and a latitude of 41.0 degrees north, extending to -71.2 degrees west and 41.85 degrees north, in accordance with the WGS84 projection. The number of grid points, the resolution of the model based on WGS84 and UTM projection are summarized in Table 4-3.

Table 4-3 SWAN Model Setting

Origin Point X (Longitude Degree)	-71.9
Origin Point Y (Latitude Degree)	+41.0
Model Resolution In X Direction (Degree)	0.00348077
Model Resolution In X Direction (Meter)	396.02
Model Resolution In Y Direction (Degree)	0.00210393
Model Resolution In Y Direction (Meter)	281.34
Number of Mesh In X Direction	200
Number of Mesh In Y Direction	400

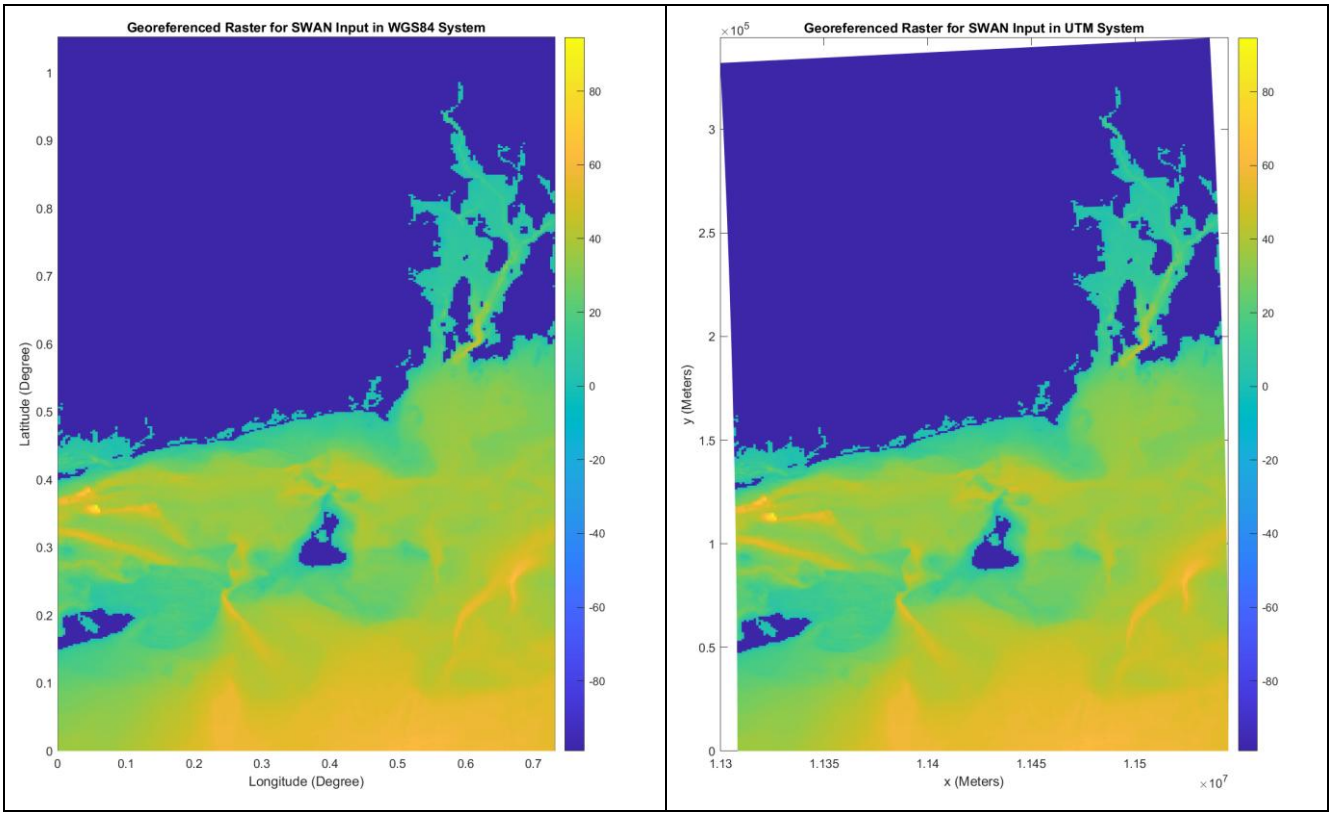

Figure 4-11. Computational domain for SWAN model based on WGS84 system (left) and UTM system (right)

SWAN Model Validation

To validate SWAN model, two scenarios are considered in this study:

- Scenario 1: Wind from Northeast: 45° Nautical Direction
- Scenario 2: Swell waves from south: 180° Nautical Direction

Scenario 1: Wind from a 45° Nautical Direction

For this scenario, an empirical equation is used, that is provided by the U.S. Army Coastal Engineering Research Center, as outlined in Volume I of the SHORE PROTECTION MANUAL (United States Army Corps of & Coastal Engineering Research, 1984). This equation determines the significant wave height, represented as "Hs" (see Equation 0-1) using the wind direction. The equation considers various parameters such as acceleration due to gravity ("g" in m/s^2), fetching distance ("F" in meters), water depth ("d" in meters), wind speed at a 10-meter elevation above sea level ("U" in m/s), and the wind speed parameterization ("UA" in m/s).

$\frac{gHs}{{U_A}^2} = 0.283 \tanh\left[0.530\left(\frac{gd}{{U_A}^2}\right)^{\frac{3}{4}}\right] \tanh\left\{\frac{0.00565\left(\frac{gF}{{U_A}^2}\right)^{\frac{1}{2}}}{\tanh\left[0.530\left(\frac{gd}{{U_A}^2}\right)^{\frac{3}{4}}\right]}\right\}$	Equation 0-1
$U_A = 0.71\,U^{1.23}$	Equation 0-2

A wind speed of 20.0 m/s at a height of 10 meters above sea level was assumed. Additionally, we set the fetching distance for the specified point, which is located at coordinates (-71.428250, 41.548556), to be 10.71 km (see Figure 4-12). Under these assumptions, the resulting significant wave height is computed to be 1.14 meters.

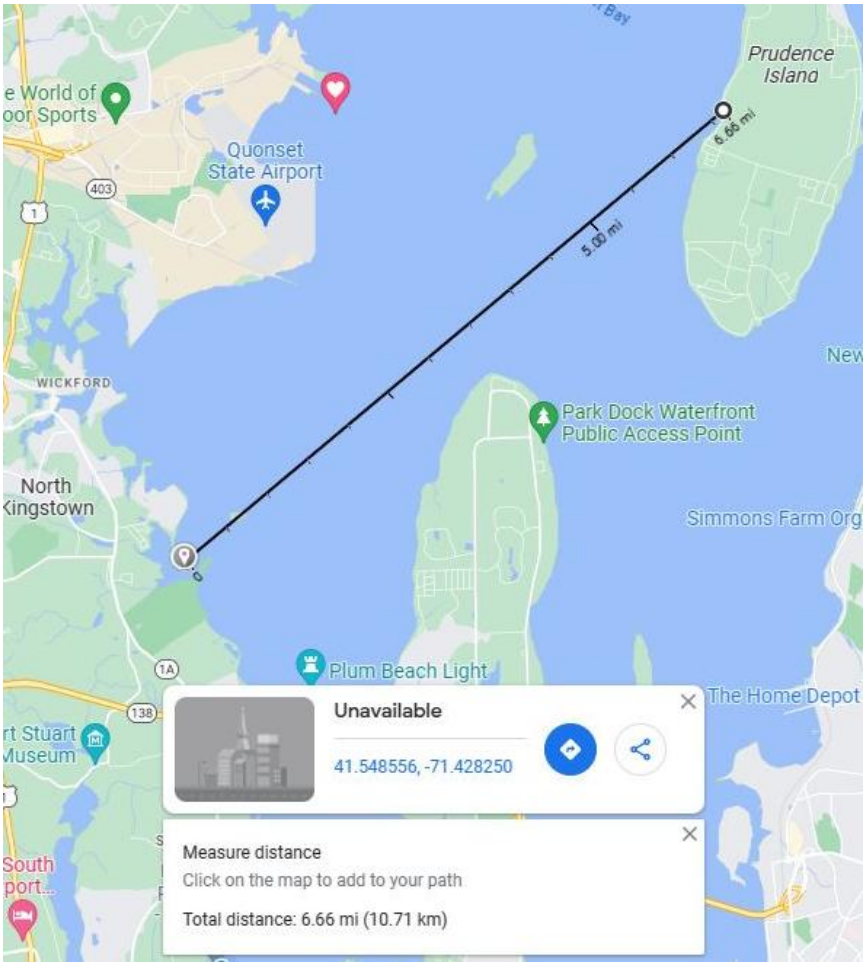

Figure 4-12. Fetch Distance (Using Google Map)

For the SWAN model, as depicted in Figure 4-13, the calculated significant wave height is 1.18 meters that closely aligns with the value calculated using the SHORE PROTECTION MANUAL equation.

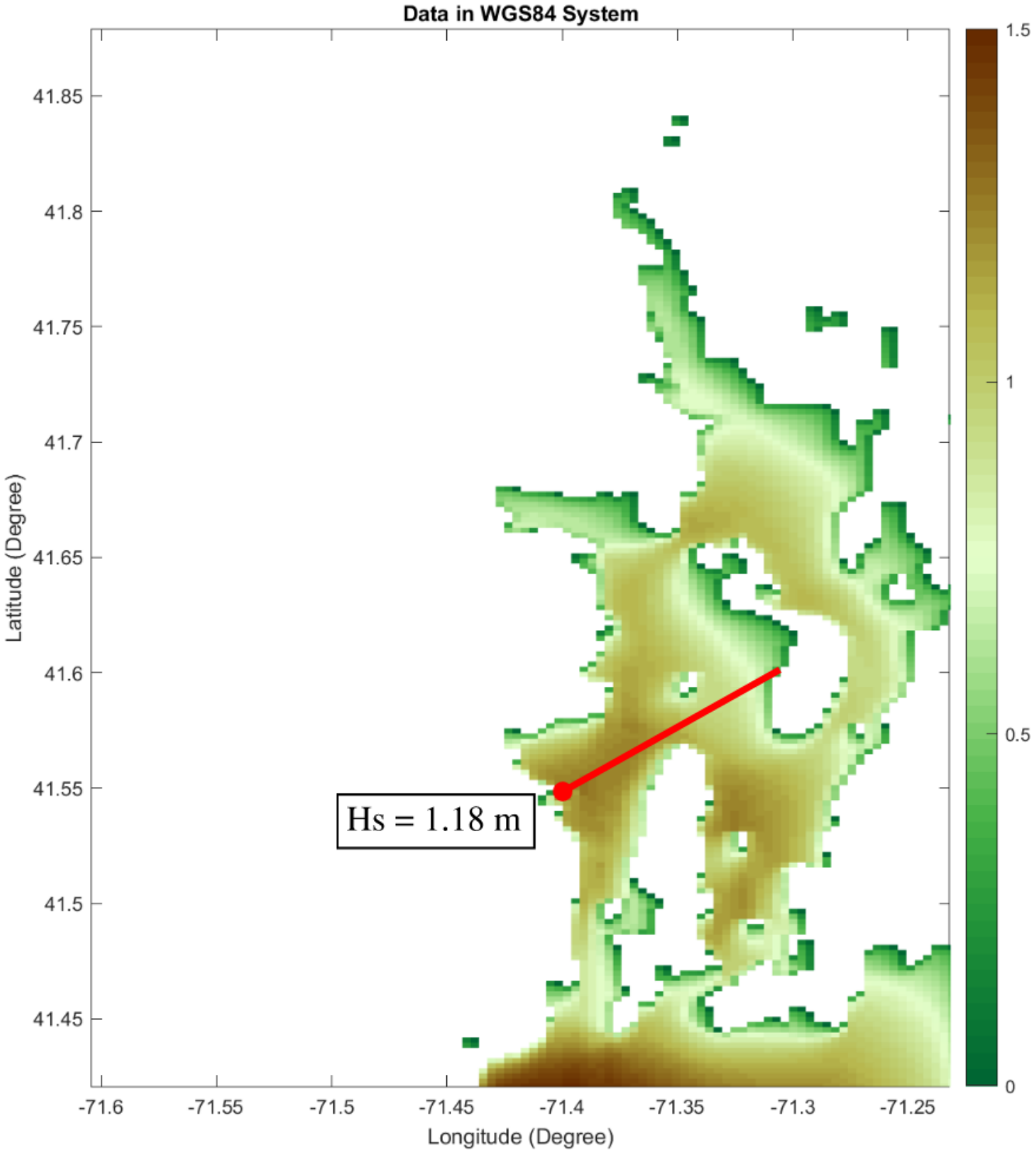

Figure 4-13. Significant Wave Height Calculated from the SWAN model by considering the scenario 1, or wind coming from northeast with the magnitude of 20 m/s.

Scenario 2: Wave from a 180° Nautical Direction

A second model assessment involving the simulation of Hurricane Irene's swell was carried out. This hurricane happened during August 21, 2011 until August 30, 2011. In this scenario, the wave height (swell)

is implemented along the southern open boundary of the domain. The hindcast wave properties were obtained from the Wave Information Study (WIS) Data Portal station ST63101 (see Figure 4-14). The wave properties are summarized in **Table 4-**. The estimated waves near the south shore of RI were compared with observed data.

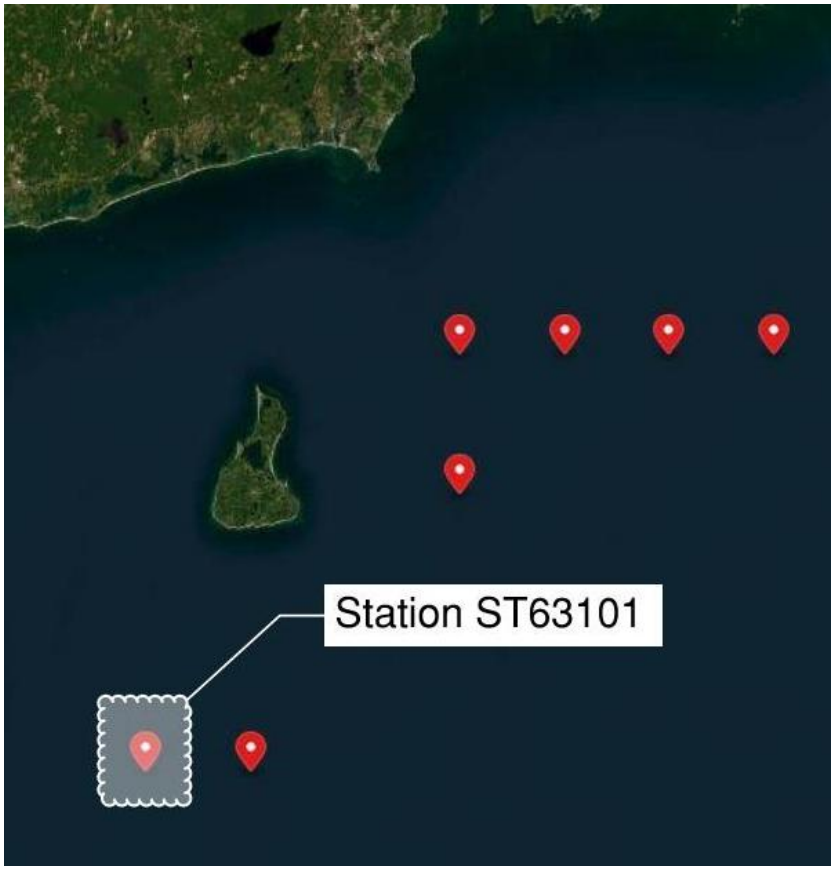

Figure 4-14. Geographical Position of The ST63101

For validation, observed data from the Rhode Island Regional Sediment Management (RI RSM) is utilized. The study includes measurement of wave properties resulting from Hurricane Irene, particularly obtained from the Center Station with the coordinates of -71.428250 longitude and, 41.548556 latitude. Based on this dataset the significant wave height for the Center Station is around four meters.

Table 4-4 Wave Parameters at ST63101 during Hurricane Irene used as boundary condition.

Significant Wave Height	Peak Period	Wave Direction
7.85	14.66	174

The significant wave height derived from the SWAN model, considering the specified boundary conditions, is illustrated in Figure 4-15. The calculated significant wave height by SWAN has 10% error at the Center Station. The modeled wave height at this station is 3.6 meters at peak compared with 4 m observed data. This discrepancy can be attributed to the absence of the wind surface boundary condition in the model's current configuration and other model errors.

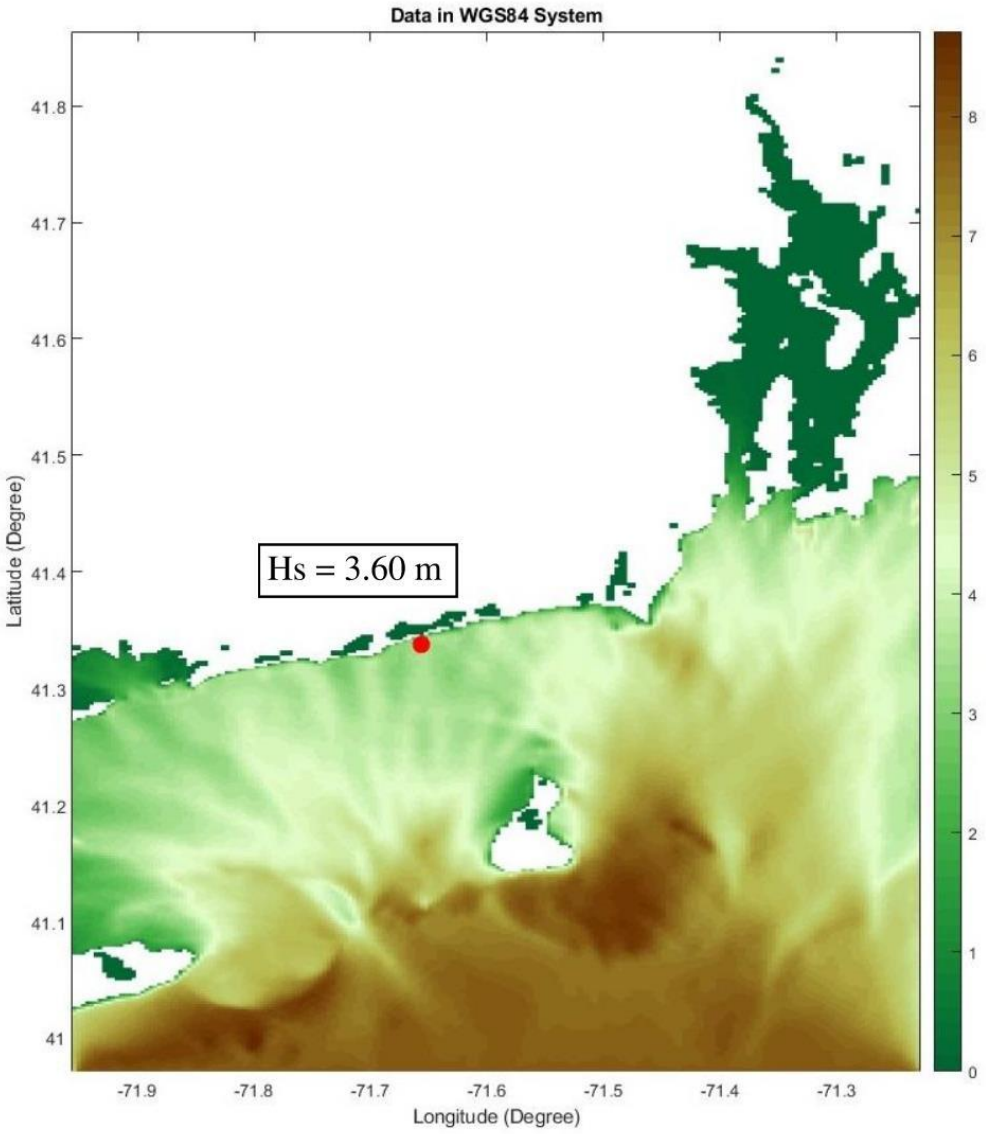

Figure 4-15. Significant Wave Height for The Second Scenario

Wave Modeling Conclusion

A wave model has been developed for the study area. The model can simulate swells either coming from the south, or wind-generated waves in Narragansett Bay and can be used for modeling wave forcing on the beach and assessing mitigation scenarios.

XBeach Model

To simulate nearshore hydrodynamics, sediment transportation, and coastal erosion, the XBeach model was utilized. This section discusses the topo/bathymetry data, its resolution, data correction, and the model setup.

Topo/Bathymetry

The area of study (Little Beach) for XBeach simulation is shown in Figure 4.16. For this study, CUDEM[1] dataset is used for the very initial step of modeling. The dataset is specifically focusing on the Ninth Arc-Second Resolution Bathymetric-Topographic Tiles. The specification of the dataset is summarized in Table 4-5.

Table 4-5 Detailed Specification of The Topo/Bathymetry Data Used in The XBeach Model

Projection	UTM[2]
Datum	NAD83[3]
File Format	GeoTIFF
Output Resolution	3.00 Meters
Vertical Datum	NAVD88[4]

In preparation for XBeach analysis, a localized domain was chosen to align with the coastal shoreline. A MATLAB script was employed to import the original raster dataset, and subsequently, the local raster data was mapped on the XBeach domain. Figure 4-17 illustrates both the parent and localized raster data within the shaded region.

[1] Continuously Updated Digital Elevation Model

[2] Universal Transverse Mercator coordinate system

[3] The North American Datum of 1983

[4] North American Vertical Datum of 1988

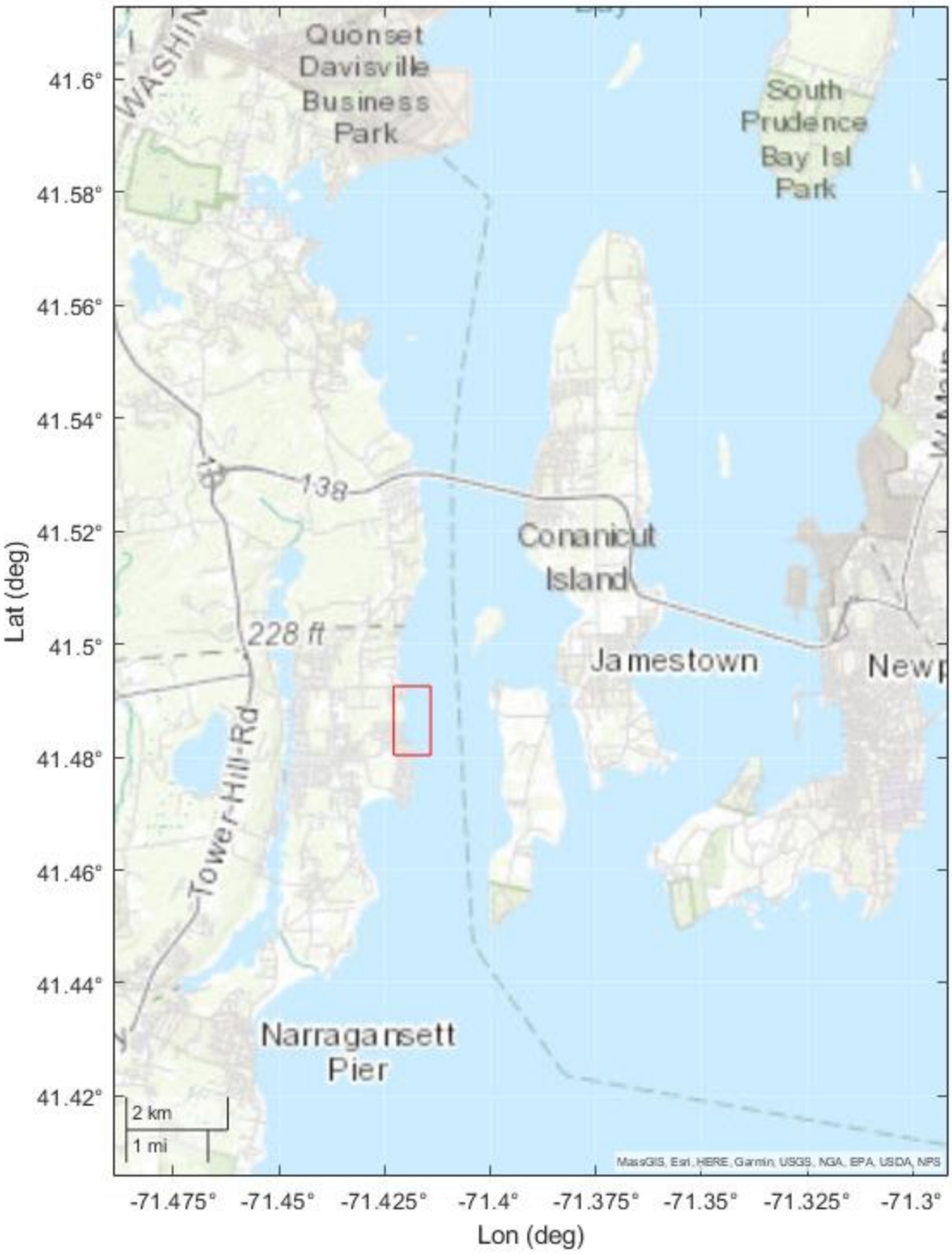

Figure 4-16. Geographical Location of Study Area, shown by the red rectangle.

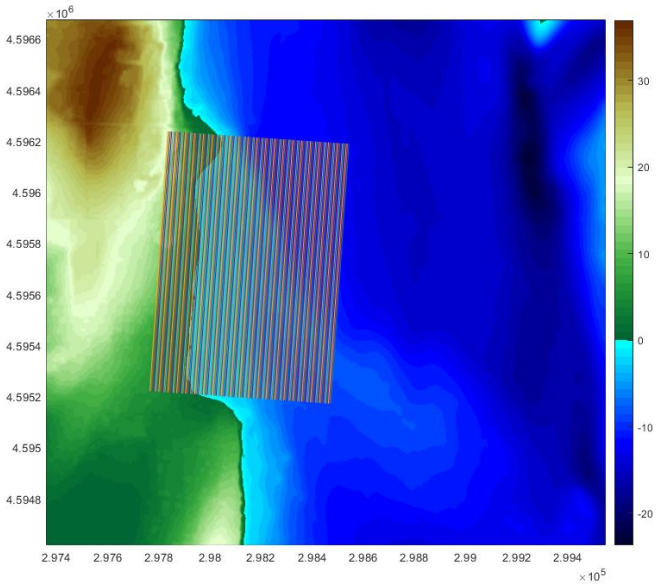

Figure 4-17 MATLAB Parent and Local Domain (Shown with Shaded Area)

It should be mentioned that the values of bathymetry are positive down by XBeach default in contrast to Figure 4-18. A correction was implemented.

Bathymetry smoothing

Due to the rapid and extreme variations observed in the bathymetry data, the model encounters instability. To mitigate this instability, we employed a smoothing technique by applying a low-pass Butterworth filter to the bathymetry data.

This approach operates on a 3D dataset and involves the specification of filter parameters such as Cutoff Frequency, Sampling Frequency, Normalized Cutoff, and Filter Order. 3D plot is generated, superimposing the original and filtered data to demonstrate the filtering's efficacy in reducing data noise, resulting in a smoother and more stable numerical simulation. These parameters should be selected in a way that does not compromise the bathymetry too much at the expense of computational efficiency.

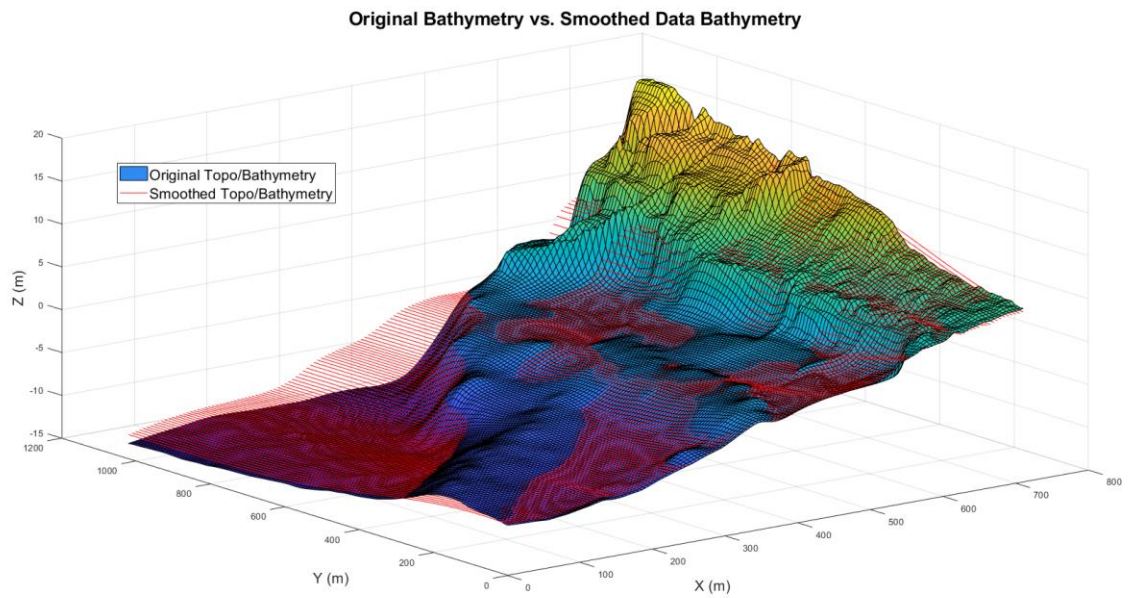

Figure 4-18 Comparison of Original and Smoothed Topo/Bathymetry Data

Grain size

We extracted the D90 and D50 metrics from the study titled " Narragansett Town Beach Replenishment Feasibility Project." Figure 4-19 shows the grain size in Narragansett Beach. Based on Figure 4-19 , the averaged D90 and D50 are 0.48 mm and 0.26 mm respectively.

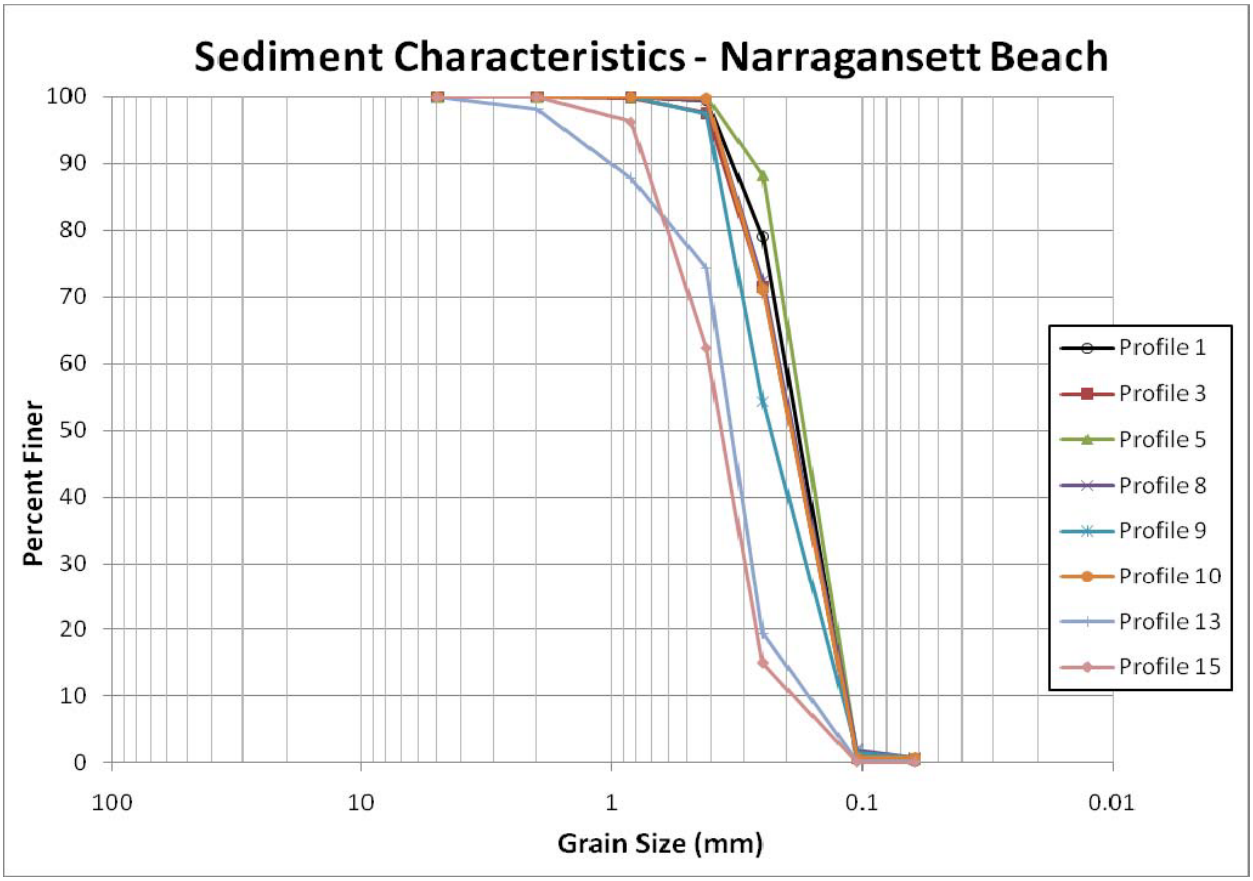

Figure 4-19. Grain Size in Narragansett Beach from Narragansett Town Beach Replenishment Feasibility Project

XBeach Model Setup

For this XBeach model, a local topo/bathymetry data is setup based on . The local domain starts from 297764.8 in x and 4595219.8 in y direction in UTM T19 zone. The local domain stretches 720 m and 1020 m in local x and y directions, respectively. The number of grid points, the resolution of the model is shown in **Table 4-**.

Table 4-6 XBeach Model Resolution

Model Resolution In X Direction (Meter)	5.00
Model Resolution In Y Direction (Meter)	7.50
Number of Mesh In X Direction	142
Number of Mesh In Y Direction	136

XBeach Results

Several scenarios were simulated. In the first step, the simulations are done only for wave boundary condition, and no currents are considered. The boundary condition for the waves is forced by the Jonswap Spectrum. The duration of the spectrum is considered for 1800 second (half an hour). Simulations were carried out for significant wave heights from Hm0 = 1.00 m to Hm0 = 7.00 m. Other parameters of the Jonswap spectrum are detailed in Table 4-7.

Table 4-7 Jonswap Spectrum Boundary Condition Variables

Significant Wave Height (Hm0)	1.00 – 7.00 m
Peak Period (Tp)	12 s
Main wave angle (mainang)	270 degrees to Nautical
Peak enhancement factor (gamma)	3.3
Directional Spreading Coefficient (s)	20
Highest frequency used to create JONSWAP spectrum (fnyp)	1.0

Three distinct sections within the model domain were selected to show the results. These sections are denoted as Section 1, Section 2, and Section 3, with their respective locations at distances of 250 meters, 500 meters, and 750 meters along the local domain's y-axis (Figure 4.20). The changes of the section profiles for different Hm0 are shown in Figure 4-21.

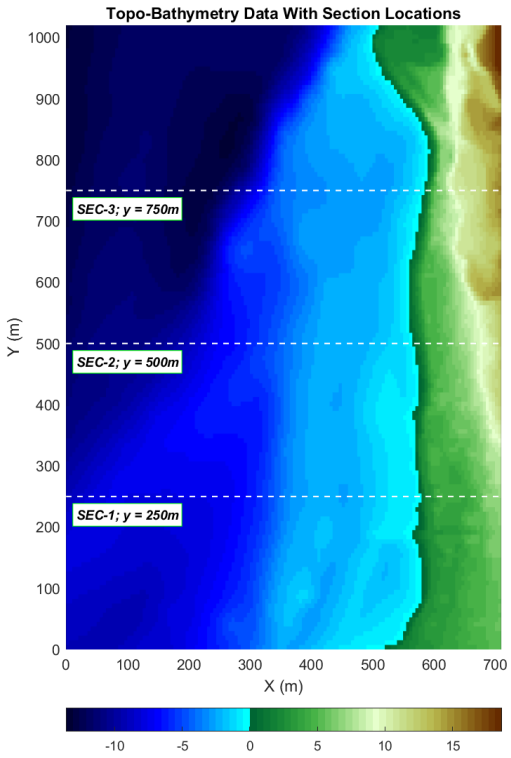

Figure 4-20. Section Cuts Locations.

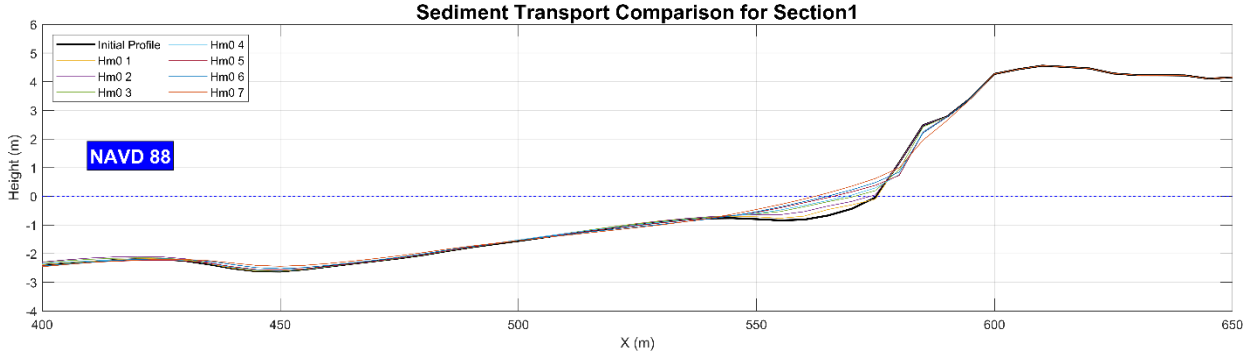

a) Bed Level Changes, Section 1

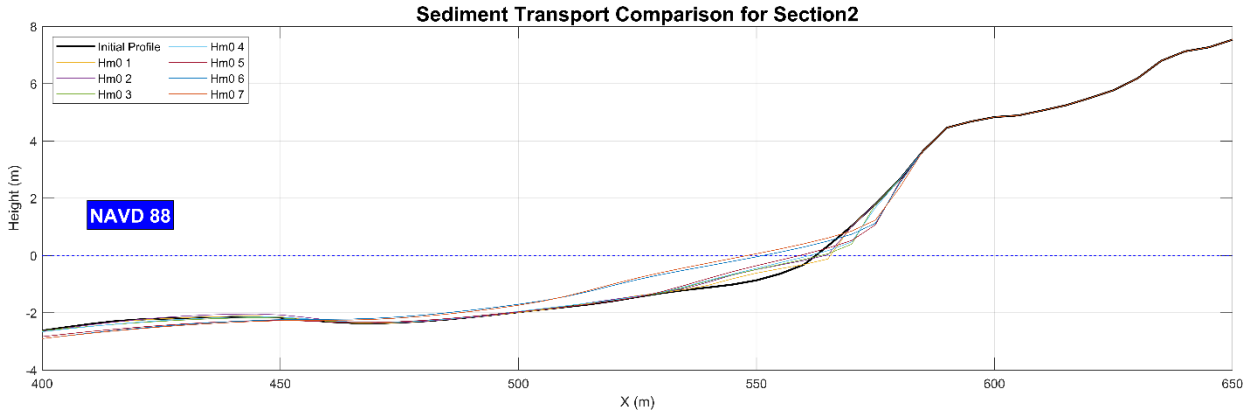

b) Bed Level Changes, Section 2

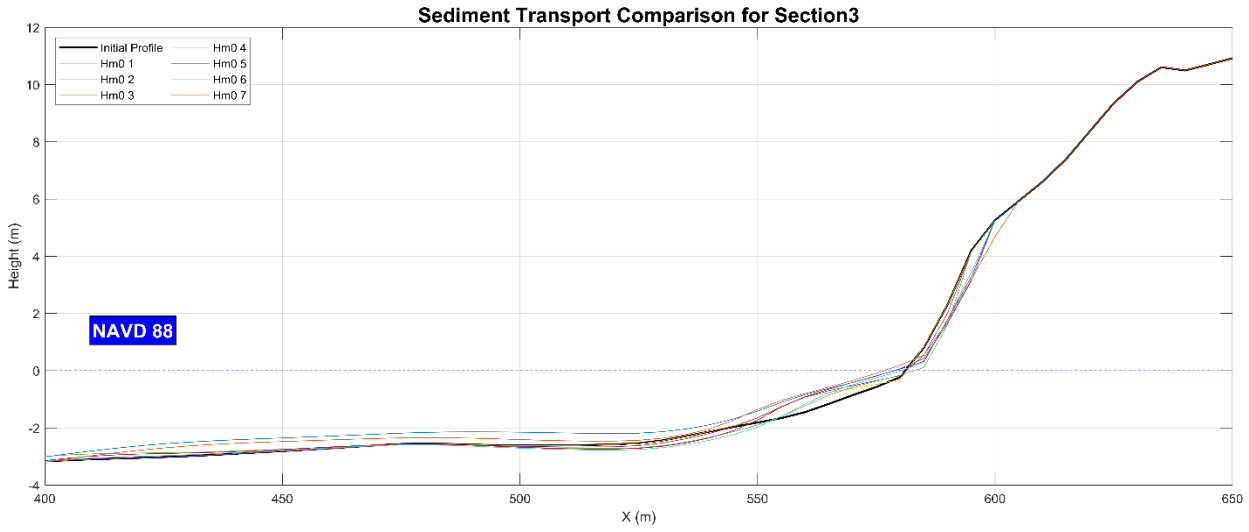

c) Bed Level Changes, Section 3

Figure 4-21. XBeach results corresponding to Hm0.

The results qualitatively show a typical pattern of erosion and sedimentation resulting from wave impact. Existing revetments and hard structures near the dune have an impact on these erosion estimates and can be further simulated by using a non-erodible surface. Further data collection, including topo-bathymetric data before and after a storm, can help further tune and validate the XBeach model. Nevertheless, the developed XBeach model, as a standard modeling tool, can be used to assess how a mitigation measure will respond to an event and qualitatively evaluate the performance of a solution.

4.5 Summary of numerical modeling

We developed a standard wave and sediment transport model for the study area using SWAN and XBeach. The models have been assessed using available data. They can predict the wave height near the area resulting from a specific storm (e.g., a 20-year storm) and how the beach may respond to the wave impact. These models can be further tuned and used for the assessment of conceptual designs aimed at reducing coastal erosion. It should be noted that coastal erosion models have many assumptions and limitations, and their use should be combined with engineering judgment and other qualitative assessments. The collected wave height data can be used to further correlate offshore wind and nearshore waves, providing a unique dataset for future studies.

The model that we have developed can be used to evaluate the utility of possible engineering solutions for mitigating coastal erosion in the Little Beach area. It will be used as part of the alternatives analysis phase of any proposed engineering projects in the Little Beach area.

4.6 References

Booij, N., Ris, R. C., & Holthuijsen, L. H. (1999). A third-generation wave model for coastal regions: 1. Model description and validation. *Journal of Geophysical Research: Oceans*, *104*(C4), 7649-7666. https://doi.org/https://doi.org/10.1029/98JC02622

Ris, R. C., Holthuijsen, L. H., & Booij, N. (1999). A third-generation wave model for coastal regions: 2. Verification. *Journal of Geophysical Research: Oceans*, *104*(C4), 7667-7681. https://doi.org/https://doi.org/10.1029/1998JC900123

Roelvink, D., Reniers, A., van Dongeren, A., van Thiel de Vries, J., McCall, R., & Lescinski, J. (2009). Modelling storm impacts on beaches, dunes and barrier islands. *Coastal Engineering*, *56*(11), 1133-1152. https://doi.org/https://doi.org/10.1016/j.coastaleng.2009.08.006

United States Army Corps of, E., & Coastal Engineering Research, C. (1984). *Shore protection manual* (4th ed.). Dept. of the Army, Waterways Experiment Station, Corps of Engineers, Coastal Engineering Research Center ; For sale by the Supt. of Docs., U.S. G.P.O. Vicksburg, Miss., Washington, DC.

Woods Hole Group (2011). Narragansett Town Beach Replenishment Feasiblity Project.

5 Major Findings of Little Beach Study

Our mapping to characterize the Little Beach study area and modeling of the important erosional processes that operate in the study area have greatly increased our understanding of what actions could be (can't be) undertaken to mitigate coastal erosion within the area. We list these findings below.

The LiDAR mapping studies of the area have provided an excellent baseline characterization of the present conditions on the beach and in the adjacent landward areas that will be essential to assessing damages in a possible future major storm. They also indicate that similar to Narragansett Town Beach, Little Beach is slowly losing volume due to the combined effects of sea level rise and erosion during storms. The erosion is highest adjacent to and seaward of the revetment that protects Colonel John Gardiner Road. This type of accelerated erosion of beach sand in front of hard coastal structures is typical. One engineering option that might mitigate this erosion would involve removal of the revetment and possibly the road to provide room to reconfigure the beach profile to provide a elongated ramp on which wave energy is dissipated. This option is a major project and the design of the elongated ramp would also be limited seaward by the presence of the extensive eelgrass beds found in the side scan sonar mapping component of the project. Many current coastal projects that involve redesign of the beach profile also involve the use of submerged artificial reef structures to help dissipate wave energy.

That option would likely be limited in the Little Beach area by the combination of very high wave energy during storm events, and the presence of the eelgrass beds and the boat ramp and mooring field.

Identifying a local source of sand that can be used as a source for dredging and beach replenishment was also evaluated by our project. The bottom offshore of Little Beach is sandy but the presence of extensive eelgrass beds on the sandy bottom precludes dredging and reuse of this material. The material that can be obtained by periodic re-dredging of the boat launch and channel area can be used for beach replenishment at Little Beach but is insufficient in volume to make much difference in the face of the ongoing beach erosion.

The wave monitoring and numerical modeling that we did in this study have produced a predictive model specific to the study area that can be used to evaluate and design test a range of possible engineering solutions to help mitigate coastal erosion within the study area. URI graduate students are testing some of these options in ongoing studies.